Annu. Rev. Astron. Astrophys. 1999. 37:603–48

FAR-ULTRAVIOLET RADIATION FROM ELLIPTICAL GALAXIES

Robert W. O'Connell
Astronomy Department, University of Virginia, P.O. Box 3818, Charlottesville, Virginia 22903-0818

Key Words stellar populations, hot stars, mass loss, galaxy evolution

■ **Abstract** Far-ultraviolet radiation is a ubiquitous, if unanticipated, phenomenon in elliptical galaxies and early-type spiral bulges. It is the most variable photometric feature associated with old stellar populations. Recent observational and theoretical evidence shows that it is produced mainly by low-mass, small-envelope, helium-burning stars in extreme horizontal branch and subsequent phases of evolution. These are probably descendants of the dominant, metal rich population of the galaxies. Their lifetime UV outputs are remarkably sensitive to their physical properties and hence to the age and the helium and metal abundances of their parents. UV spectra are therefore exceptionally promising diagnostics of old stellar populations, although their calibration requires a much improved understanding of giant branch mass loss, helium enrichment, and atmospheric diffusion.

1. INTRODUCTION

Far-ultraviolet radiation was first detected from early-type galaxies by the *Orbiting Astronomical Observatory-2* in 1969. This was a major surprise because it had been expected that such old stellar populations would be entirely dark in the far-UV. To the contrary, not only did elliptical galaxies and the bulges of early-type spirals contain bright UV sources, but their energy distributions actually increased to shorter wavelengths over the range 2000 to 1200 Å, resembling the Rayleigh-Jeans tail of a hot thermal source with $T_e \gtrsim 20000$ K. The effect was therefore called the "UV-upturn," the "UV rising-branch," or, more simply, the "UVX." It was only the second new phenomenon (after X-rays from the active galaxy M87) discovered by space astronomy outside our Galaxy.

Controversy flourished over the interpretation of the UVX for the next 20 years because of the slow accumulation of high quality UV data. More recent evidence has winnowed the alternatives and strongly supports the idea that the UVX is a stellar phenomenon (as opposed to nuclear activity, for example) associated with the old, dominant, metal-rich population of early-type galaxies. It is the most

variable photometric feature of old stellar populations. It appears to be produced mainly by low-mass, helium-burning stars in extreme (high temperature) horizontal branch and subsequent phases of evolution. Such objects have very thin envelopes ($M_{ENV} \lesssim 0.05\,M_\odot$) overlying their cores. On both theoretical and observational grounds, the lifetime UV outputs of these stars are exquisitely sensitive to their physical properties. They depend strongly, for instance, on helium abundance; the UV spectrum is the only observable in the integrated light of old populations with the potential to constrain their He abundances. More remarkably, changes of only a few 0.01 $M_\odot$ in the mean envelope mass of an extreme horizontal branch population can significantly affect the UV spectrum of an elliptical galaxy.

If this interpretation is correct, then far-UV observations become a uniquely delicate probe of the star formation and chemical enrichment histories of elliptical galaxies. They do, that is, once we understand the basic astrophysics of these advanced evolutionary phases and their production by their parent populations. However, this is one of the last underexplored corners of normal stellar evolution, and a complete interpretation is not yet at hand, even for nearby systems such as globular clusters where full color-magnitude diagram information is available. The key physical process involved in producing the small-envelope stars is mass loss during low-gravity phases on the red giant branch and subsequent asymptotic giant branch. Serious modeling of mass loss has only recently begun, and we so far have little intuition for the effects of population characteristics such as metal abundance. Although the interpretation of the integrated light of galaxies has heretofore relied on astrophysics established and tested in the context of local stars, it may be that the UVX problem will be the first where observations of galaxies will act as strong diagnostics of stellar evolution theory. At any rate, it is clear that to understand the controlling mechanisms of the UVX in galaxies we must conjoin integrated light observations of distant galaxies with the stellar astrophysics of globular clusters and hot field stars in our own and nearby galaxies.

There are broader ramifications of this interpretation as well. UV light acts as a tracer for stellar mass loss. As the primary source of fresh interstellar gas and dust in old populations, stellar mass loss is directly linked to a diverse set of other important phenomena, including gas recycling into young generations of stars, galactic winds, X-ray cooling flows, far-infrared interstellar emission, dust in galaxy cores, and gas-accretion fueling of nuclear black holes. The UV light also traces the production of low-mass stellar remnants. The hot UVX stars, regardless of their origin, are important distributed contributors to the interstellar ionizing radiation field of old populations. It is possible that the UVX is influenced by, and therefore reflects, galaxy dynamics. Finally, characterization of the UV light of nearby ellipticals, its separation into young or old stellar sources, and its predicted evolution is also basic to the development of realistic "K-corrections" for cosmological applications to high redshift galaxies and to interpretation of the cosmic background light.

There has been excellent progress over the last decade in understanding the UVX phenomenon, but the first question that might occur to the reader is why

it took 30 years simply to identify its source. The answer lies in our historically limited capability for extragalactic UV observations, a subject we discuss in the next section. Following that, we describe the discovery of far-UV light from old populations and its basic observational characteristics, the lively debate over the leading alternative interpretations, and the confluence of theory and new observations that has led to the currently accepted interpretation. We also discuss several of the other observational opportunities presented by the generally faint UV background in galaxies. By "early-type" galaxies in this paper, we mean ellipticals, S0s, and the large bulges of spirals of types Sa and Sb, although most of the detailed analysis to date has concentrated on Es and S0s.

2. INSTRUMENTAL CONSIDERATIONS

Progress in understanding the far-ultraviolet radiation from galaxies has been more circumscribed by instrumental limitations than was the case, for instance, in extragalactic X-ray astronomy. Fewer long-lived ultraviolet facilities have been available, and most of these have not been well suited for the study of galaxies. The problems are both intrinsic and technical. Intrinsically, galaxies are faint, extended sources. For typical elliptical galaxies, incident far-UV photon rates per unit solid angle per unit wavelength are typically over 50 times smaller than in the V-band. The centers of nearby bright ellipticals produce only a few $\times 10^{-15}$ erg s^{-1} cm^{-2} Å^{-1} arcsec^{-2} at 1500 Å averaged over a 10 radius (Burstein et al 1988, Maoz et al 1996, Ohl et al 1998). The paucity of high contrast spectral features in UV hot star spectra at the spectral resolution and S/N possible for E galaxies has also hampered interpretation.

There has never been a large area UV sky survey sensitive enough to detect galaxies. The only all-sky survey yet made in the UV was by TD-1 in 1973 (Boksenberg et al 1973). This has a limit of about 9th magnitude and did not include a single galaxy or QSO. The GALEX mission (Martin et al 1997), now under development, will remedy this situation and produce a survey up to 10 magnitudes fainter. For now, however, the fact remains that the deepest survey of the UV sky is comparable to the Henry Draper catalog of stars, made around 1900. So UV astronomy, at least in this sense, is still 100 years behind optical astronomy.

The technical development of UV instrumentation has been reviewed by Boggess & Wilson (1987, spectroscopy), O'Connell (1991, imaging), Joseph (1995, detectors), and Brosch (1998, surveys). UV telescopes have been small, mostly less than 40 cm diameter. Other than the 2.4-m Hubble Space Telescope (HST), the largest UV instrument available has been the 1-m diameter *Astro* Hopkins Ultraviolet Telescope (HUT), which as a Shuttle-attached payload had an equivalent dedicated observing lifetime in 2 missions of only about 6 days (Kruk et al 1995). Observations of galaxies are difficult with the small entrance apertures available on most UV spectrometers, for example the International Ultraviolet Explorer (IUE) ($10'' \times 20''$) or the HST/Faint Object Spectrograph ($\leq 1''$), which

were designed for point sources. With IUE, long exposures of typically 4–8 hours were needed to register far-UV spectra of galaxies. Newer instruments are better matched to requirements for galaxy work. HUT was the first UV spectrometer designed specifically for galaxies, with apertures as large as $19'' \times 197''$ (providing, however, only one spatial resolution element). The *Astro* Ultraviolet Imaging Telescope (UIT) experiment, designed for filter imaging in the 1230–3200 Å region, had a field of view ($40'$) and spatial resolution ($3''$) well matched to ground-based studies of nearby galaxies. The new Space Telescope Imaging Spectrograph (STIS) offers UV apertures up to $2'' \times 52''$, encompassing many spatial resolution elements, and can image $25'' \times 25''$ fields with UV photon-counting detectors and $0.05''$ resolution. The HST Advanced Camera for Surveys, scheduled for installation in 2000, has high throughput UV cameras with fields up to $30'' \times 30''$.

The quantum efficiencies of UV detectors such as cesium iodide and cesium telluride photocathodes are only modest (10–30%), and net throughputs are further compromised by the lower reflectivities and transmissions of UV optical components. The most widely used mirror coating, magnesium fluoride, has a short-wavelength cutoff near 1150 Å. To obtain response to the Lyman discontinuity at 912 Å special coatings such as silicon carbide are now available (e.g. Kruk et al 1995), though these do not achieve reflectances typical of standard coatings at longer wavelengths.

Two special requirements for far-UV observations have serious practical consequences. First is the necessity to suppress the effects of the strong geocoronal Ly-α emission line at 1216 Å. This is usually straightforward in spectrographs, but in photometers or imagers the only remedy is to use blocking filters that permit response only for $\lambda \gtrsim 1250$ Å. Second is the necessity to suppress residual filter and detector response to long-wave ($\lambda > 3000$ Å) photons. Even though this may be only a tiny fraction of peak UV response, it covers a wide wavelength range. Because cool sources, such as stars with $T_e < 7000$ K, can have optical f_λ thousands of times higher than their UV f_λ, there can be serious "red leak" contamination of UV observations. Despite considerable effort (e.g. on Wood's filters), it has not been possible to develop fully satisfactory long-wave blocking devices with good peak UV response. Therefore, red leak suppression depends on the use of "solar-blind" detectors with large photoelectron work functions, such as cesium iodide, which has very small response for $\lambda > 1800$ Å. Such detectors have been used in most UV spectrometers but were not available in the HST Wide Field Camera (WFPC2) or HST Faint Object Camera (FOC), both of which consequently required careful red leak calibrations for use shortward of 2500 Å. The effects of red leaks on HST photometry of stars and galaxies can be dramatic and have been discussed by Yi et al (1995) and Chiosi et al (1997). The requirements for simultaneous Ly-α and red leak suppression imply smaller bandwidths and lower throughputs for far-UV imaging or photometry than is typical at longer wavelengths.

Because of these technical constraints, the working "far-ultraviolet" (FUV) band covers ~1250–2000 Å for imaging or photometry, extended to about 1150 Å for spectroscopy. The "mid-ultraviolet" (MUV) band covers ~2000–3200 Å

(3200 Å being both the useful sensitivity limit of cesium telluride photocathodes and the short-wavelength cutoff of the Earth's atmosphere). We will call the 3200–4000 Å region accessible from the Earth's surface the "near-ultraviolet" (NUV). The 912–1150 Å region in galaxies has been explored to date only by HUT, though FUSE (launched in 1999) will also cover this range in brighter objects.

Unless noted, magnitudes quoted in this paper will be on the monochromatic system, where $m_\lambda = -2.5 \log F_\lambda - 21.1$ and F_λ is the mean incident flux in the relevant band in units of erg s^{-1} cm^{-2} $Å^{-1}$; the zero point is such that $m_\lambda(5500\ Å) = V$. Notation for colors will be, for instance, $1500–V \equiv m_\lambda(1500\ Å)–V$.

3. DISCOVERY AND ALTERNATIVE INTERPRETATIONS

Prior to the first UV observations, there was a widespread expectation that normal elliptical galaxies would be uninteresting in the FUV (as, later, would also be the case with the X-ray and far-infrared regions). The hottest identified stellar component of any consequence was the main sequence turnoff, with a temperature ($T_e \sim 6000$ K) too cool to produce many FUV photons. Although it was recognized that the old, metal-poor populations of globular clusters sometimes contained horizontal-branch (HB) stars with $T_e \gtrsim 10000$ K, these were thought to be absent in the clusters (e.g. 47 Tucanæ) with metal abundances nearest those of massive galaxies. The only hint of hot populations in E galaxies was the presence of [O II] emission lines, though these could plausibly be explained without stellar photoionization (Minkowski & Osterbrock 1959).

FUV radiation from galaxies was first detected by the University of Wisconsin UV photometer carried on the second *Orbiting Astronomical Observatory* (OAO-2). The experiment obtained fluxes with an entrance aperture of $10'$ diameter in 7 intermediate band filters extending from 4250 Å to the FUV at 1550 Å. The first announcement (Code 1969) of results for an old population was for the central bulge ($r < 900$ pc) of the Local Group Sb spiral M31. As expected, the energy distribution of M31 fell steeply between 3500 and 2500 Å but then, remarkably, began to rise again at shorter wavelengths. A more recent UV-optical spectrum of M31 is shown in Figure 1. Since the energy distributions of normal stars cooler than $T_e \sim 8500$ K (spectral type A5) decline precipitously below 1800 Å owing to absorption by metallic ionization edges (e.g. Fanelli et al 1992), the detection of any far-UV flux in galaxies implies sources with higher equivalent temperatures. After a difficult calibration process, OAO-2 photometry was ultimately published for 7 E/S0 objects and the M31 bulge (Code et al 1972, Code & Welch 1982). The OAO-2 detections of two objects were confirmed, and new detections made of another 11 E galaxies, by the *Astronomical Netherlands Satellite* (launched in 1974) using intermediate band photometry with a $2.5' \times 2.5'$ aperture over the range 1550–3300 Å (de Boer 1982).

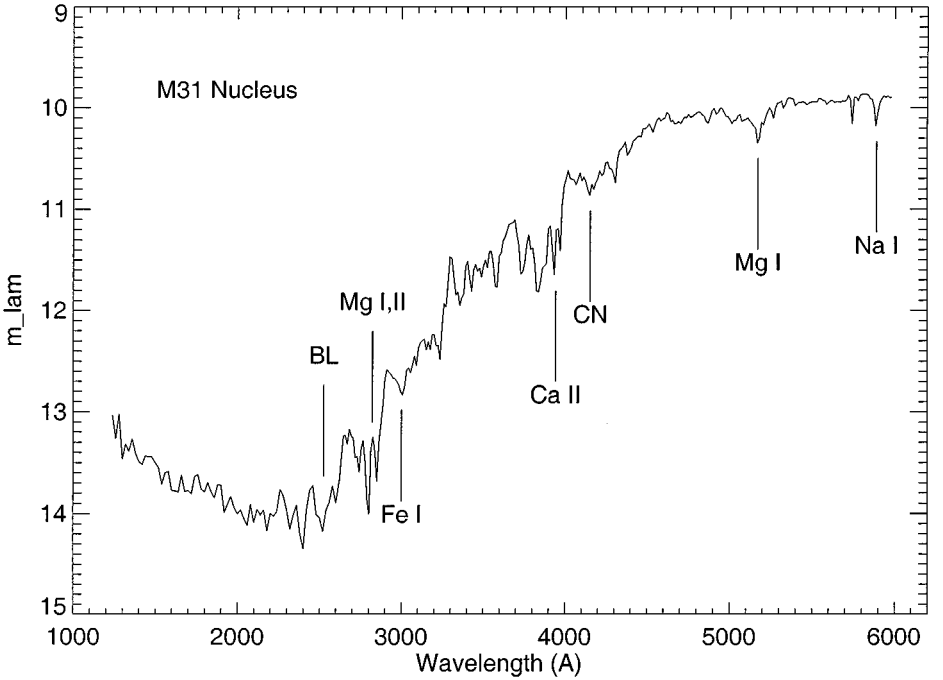

Figure 1 A composite UV-optical energy distribution for the center of the Sb galaxy M31. IUE data taken with a $10'' \times 20''$ aperture is plotted below 3200 Å, while a ground-based spectrum covering the same region is plotted above. Resolution is 20 Å below 2600 Å and 12 Å above. Irregularities in the UV spectrum below 2200 Å are mainly noise. Some of the stronger absorption line features are identified ("BL" corresponds to a strong blend of Fe and other metallic lines near 2538 Å). The "UV-upturn" is the rise in the spectrum at wavelengths shorter than 2000 Å. By simple extrapolation of the far-UV continuum slope, one finds that the upturn component contributes only about 0.3% of the V light of the galaxy. Spectrum courtesy of D Calzetti.

An immediate conclusion from the UVX observations which was emphasized by Code and his colleagues was that early-type galaxies exhibited much larger scatter in the UV than was expected from their conspicuously homogeneous behavior in the optical to near-IR (4000–20000 Å) region. The UV observations implied divergent histories at some level and were among the first indications that elliptical galaxy populations were more heterogeneous than envisioned in Baade's classic definition of Population II (Baade 1944, O'Connell 1958, O'Connell 1980, Faber et al 1995). They called into question the use of E galaxies as "standard candles" in cosmological studies. They also complicated the construction of accurate K-corrections needed to transform photometry of high redshift elliptical galaxies to standard bands in the restframe (e.g. Pence 1976, Coleman et al 1980, King & Ellis 1985, Bertola et al 1982, Kinney et al 1996).

Interpretation of the unexpected OAO-2 results was initially confused by calibration uncertainties which produced anomalously steep FUV energy distributions (in normal spirals and irregulars as well as early-type systems, see Code & Welch 1982). Code (1969) and Code et al (1972) suggested that the UVX component was nonthermal radiation from an active nucleus (AGN) or scattering of photons from massive hot stars by interstellar dust. The latter would have implied that most E/S0 galaxies contain an appreciable Population I component.

Hills (1971) pointed out that the steep rise of the M31 UV spectrum to higher photon energies was incompatible with known nonthermal sources but was closely matched by the Rayleigh-Jeans tail of a high temperature thermal source. Based on comparison with a small sample of UV-bright stars in the globular cluster M3, he proposed that the UV upturn is produced by highly evolved, hot, low-mass stars such as the central stars of planetary nebulae, now known as post-asymptotic giant branch (PAGB) stars, or their hot white dwarf descendents. He did not require that these be members of a strong Population II (old, metal-poor) component but pointed out that their prominence would probably depend on metal abundance.

Tinsley (1972a) argued that the UV light arose instead from young, massive, main sequence stars and showed that a spectral synthesis model for an old galaxy with an exponentially declining star formation rate and an e-folding time of 2 Gyr could fit the OAO-2 flux for M31 observed at 1700 Å. This would imply that the UVX was related to a normal, if temporally extended, star formation process in early-type systems. Fuel for the star formation might be primordial gas consumed gradually over a Hubble time, mass loss from red giants, or material accreted from outside galaxies (Gallagher 1972, Tinsley 1972b, O'Connell 1980, Gunn et al 1981). Residual star formation histories of the type suggested by Tinsley would drastically change the predicted properties of E galaxies viewed at moderate look-back times, whereas the low-mass star interpretation would have less serious implications for spectral evolution.

It was implicit in these early studies that the hot components that dominated the far-UV light could be virtually undetectable at visible wavelengths—i.e. that the UV was providing entirely independent information about galaxies. Ignoring any contribution from the cool components to the UV light, the maximal fractional contribution of a hot component to the integrated V-band light of a galaxy will be $p_{max} \sim 10^{0.4\,\Delta}$, where $\Delta = (1500\text{–V})_{\rm hot} - (1500\text{–V})_{\rm obs}$. A color for a typical E galaxy is $(1500\text{–V})_{\rm obs} \sim +3$ while a component with an appropriate far-UV spectral slope (B0 equivalent) has $(1500\text{–V})_{\rm hot} \sim -4.5$, implying that $p_{max} \sim 0.001$. This is about 50 times smaller than could be directly detected in the V-band using spectral synthesis techniques.

The early workers on the UVX realized that the best tests of the alternative interpretations were (*a*) UV spatial structure and (*b*) UV spectral features observed at higher resolution. An active nucleus would be a concentrated point source, whereas a population of low-mass stars would presumably have a smooth distribution similar to that found in the optical bands for bulges and E galaxies. Young, massive-star populations would likely have a clumpy structure, similar to the OB associations found in spiral arms, and they might well be concentrated to disks. In nearer

galaxies individual massive OB stars could be isolated. Spectroscopically, a UV-bright AGN would be easy to identify on the basis of broad, high-excitation emission lines. Active massive star-forming regions characteristically exhibit strong UV resonance lines of Si IV, C IV, and other species, often with P-Cygni profiles (e.g. Kinney et al 1993), whereas the spectra of hot, low-mass stars are relatively weak-lined in the 1200–2000 Å region.

Because of limited UV observing opportunities, it would not be possible to apply these tests in a definitive way until over a decade after the discovery of the UVX. Only short-duration sounding rocket or balloon experiments were available until 1978. The most productive observing facility for the study of the UVX in the period 1978–1990 was IUE (Kondo 1987). IUE's handicaps of small effective collecting area, small entrance aperture, and limited dynamic range were beautifully compensated by its record 18 year lifetime and a capability for very long integration times, and it produced an invaluable set of UVX spectra. The fact that its point spread function was smaller than its $10'' \times 20''$ entrance aperture also meant that spatial structure could be studied to a radius of $10''$. After 1990, HST and the two *Astro* missions provided new capabilities to study the UVX.

In the next two sections, we describe the basic phenomenology of far-UV sources in bright early-type galaxies, as determined by IUE and other instruments, and how this bears on the now accepted interpretation of these as low-mass stars in old stellar populations.

4. SPATIAL STRUCTURE OF THE UVX

4.1 Evidence Against Young Stars

UV imaging of early-type galaxies began in the 1970s. Early rocket and balloon experiments obtained low S/N images of the central bulge of M31 which showed that it was an extended source in the far-UV with $r \gtrsim 4'$ (Deharveng et al 1976; Carruthers et al 1978; Deharveng et al 1980). This was sufficient to exclude the AGN interpretation (in this particular case) but could not readily distinguish between the old and young star models or other types of diffuse sources. A later rocket imaging experiment by Bohlin et al (1985) provided far- and mid-UV photometry of M31 with $20''$ resolution. The UV intensity profiles of the bulge were smooth and similar to Kent's (1983) R-band profile for $r \lesssim 1.1'$. Although localized regions of massive star formation were readily detectable in the outer spiral arms, similar structures were absent in the bulge, nor could individual bright OB stars be detected there.

IUE observations of bright early-type galaxies (including M31, M32, NGC 3379, NGC 4472, M87, NGC 4552, and NGC 4649) confirmed the spatial extension of the far-UV light, even in the case of the prominent AGN of M87, and indicated that it paralleled the profile of the visible light, at least over the innermost $10''$ (Bertola et al 1980, Perola & Tarenghi 1980, Nørgaard-Nielsen & Kjærgaard 1981, Oke et al 1981, Bertola et al 1982, O'Connell et al 1986). Deharveng et al

(1982) and Welch (1982) used multiple IUE spectra to study the light distribution within the inner 15″ of the M31 bulge. They obtained a smooth profile, unlike those of star-forming regions, but found that the FUV light was slightly more concentrated to small radii within this region than MUV or B band light, producing gradients of several 0.1 mags in colors. The smooth distribution of UVX light in these cases and its similarity to the optical band profile, where old stars dominate, strongly suggested that old stars produced the UVX.

In another rocket experiment, Onaka et al (1989) and Kodaira et al (1990) obtained low-resolution, wide-field UV images of the Virgo cluster, extending the earlier photometry of Smith & Cornett (1982) at 2400 Å to 1600 Å. By comparing their total fluxes with IUE values for the nuclei, Kodaira and colleagues found evidence of large UV color gradients in five Virgo E galaxies. They attributed the blue nuclear excesses and the observed scatter in 1500–V colors to recent star formation from galactic cooling flows, though their observations were also consistent with gradients in low-mass populations.

The best available set of large area UV maps of early-type galaxies was obtained by the *Astro* UIT experiment during two Space Shuttle missions in 1990 and 1995 (Stecher et al 1997). Twenty-two ellipticals and early-type (S0-Sb) spiral bulges were imaged with good S/N at 3″ resolution, and results for 10 of these have been published (O'Connell et al 1992, Ohl et al 1998). UIT images of two Fornax cluster elliptical galaxies are shown in Figure 2. In the best cases, it was possible to obtain UV surface brightness profiles to $\mu_\lambda \sim 27$ mag arcsec^{-2}. All of

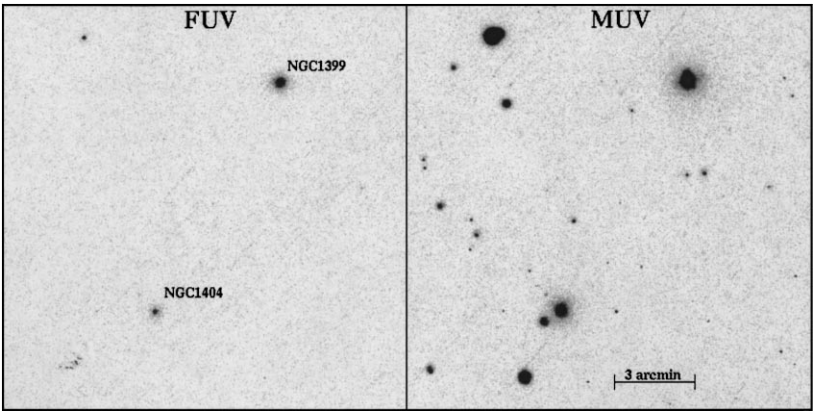

Figure 2 *Astro*/UIT images of the Fornax cluster ellipticals NGC 1399 and 1404 in broad bands in the far-UV (1500 Å) and mid-UV (2500 Å) with spatial resolution of $\sim$3″. The mid-UV band is dominated by the main sequence turnoff. All of the far-UV light is from the UVX component. It is smooth, without evidence for massive stars, though is more concentrated than the mid-UV light. NGC 1399 has one of the strongest UVX components yet discovered. Note that the foreground stars have mostly vanished in the FUV band; this is a pictorial representation of how unusual are the objects which make up the UVX.

the objects exhibit smooth UV profiles (except M87, in which the nonthermal jet is bright), with none of the clumpiness normally associated with recent massive-star formation, and the FUV contours are consistent in shape and orientation with optical-band isophotes. There is little evidence for dust lanes or clouds in the galaxy centers; such features should be readily detectable because of the high selective UV extinction of normal dust. In the M31 bulge, the point source detection threshold was $m_\lambda(2500\ \text{Å}) \sim 18.4$, which excluded the presence of individual main sequence stars hotter than B1 V (O'Connell et al 1992). Over 200 such objects would be expected in the central $2'$ of the bulge if massive stars formed with a normal initial mass function produced the FUV light. The FUV profiles of about half the sample are well fitted by de Vaucouleurs functions ($\mu \sim a + br^{0.25}$), which are characteristic of spheroids at optical wavelengths. However, the inner FUV profiles of several objects (NGC 3379, 4472, and 4649) are more consistent with an exponential function (Ohl et al 1998). Although exponentials are normally associated with disks, the FUV isophotal contours are congruent to the B-band contours, and the 3-dimensional FUV light distributions are therefore unlikely to be genuinely disklike. (Because of the large UV/optical color gradients discussed below, it is not necessarily expected that the UV profiles of objects that are true spheroids at optical wavelengths would be closely de Vaucouleurs in shape.)

High-resolution UV imaging from HST (mainly of smaller $\leq 22''$ nuclear fields with the FOC) has confirmed the absence of massive stars in the centers of M31 and M32 (King et al 1992, Bertola et al 1995, King et al 1995, Cole et al 1998, Brown et al 1998a, Lauer et al 1998) and in most UVX sources in the nuclei of 56 early-type galaxies in the 2300 Å survey of Maoz et al (1996).

The collective evidence of all these structural studies is that the far-UV light in most early-type galaxies originates in a stellar component with dynamics characteristic of the bulk of the old stellar population. Active nuclei or young massive stars are not important in most cases.

4.2 Structural Variations

However, the UV-bright population is not a simple extension of the well-studied, optically bright one. This was evident from the scatter in the ratio of UV to optical light first reported by Code et al (1972) and Code & Welch (1982), which has been amply confirmed by later observations (see Section 5.2). In addition, large internal gradients in UV/optical colors have been revealed in almost all cases studied with sufficient S/N. Five of the galaxies shown in Figure 3 from the Ohl et al (1998) UIT sample display large internal 1500–B color gradients with net changes up to $\sim$1.0 mag over the region photometered. The 1500–B colors of 7 of the 8 objects become redder outward, meaning that the far-UV light is more concentrated to the galaxy centers than the optical light. Both in amplitude and sign, these changes are dramatically unlike the very mild, bluer-outward color gradients encountered in the optical and IR (e.g. Peletier et al 1990). M32 is the only object which becomes bluer in 1500–B at larger radii.

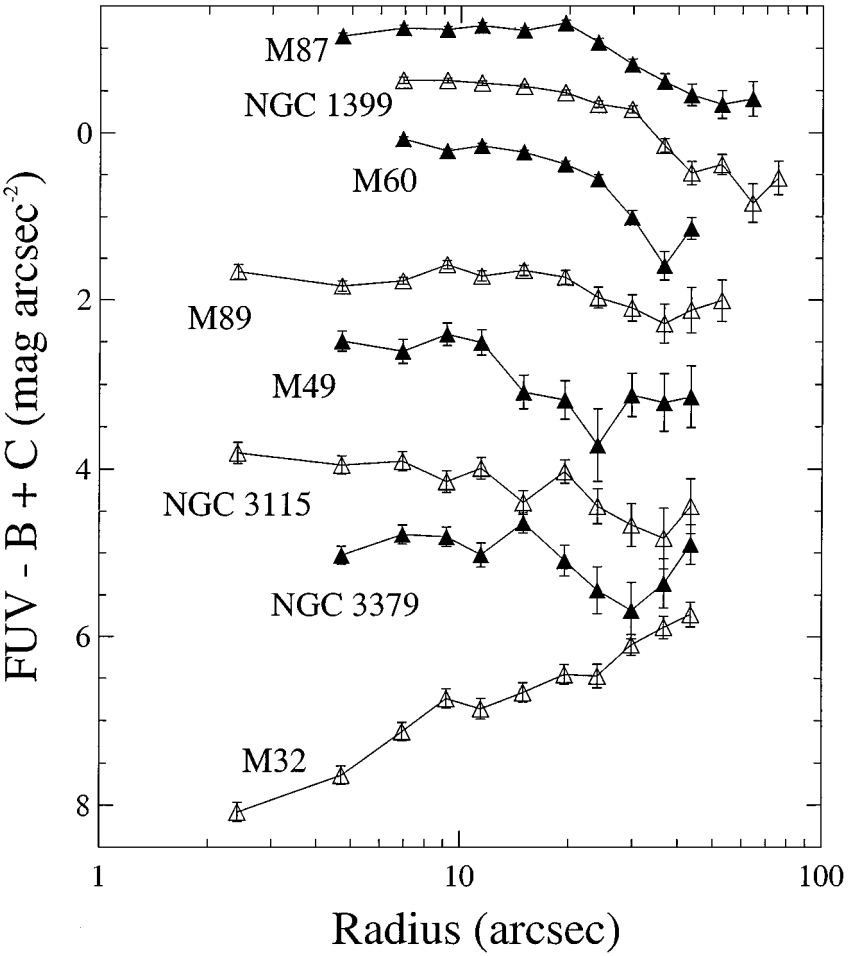

Figure 3 Radial FUV–B color profiles for 8 early-type galaxies obtained by comparing *Astro*/UIT far-UV surface photometry with B-band data from the literature. The curves have been offset for clarity and arranged in order of increasing central UVX. One sigma error bars are shown. FUV–B colors redden with increasing radius in all cases except M32, which shows a strong, reversed profile. It is the only object currently known to have this behavior. There is an interesting two-component structure in most of the profiles. Offsets in order from the top down are $C = -2.5, -2.0, -1.5, 0.0, 0.0, +1.0, +2.0$, and $+3.5$ mag arcsec^{-2}. From Ohl et al (1998).

Internal extinction by dust cannot be responsible for these gradients. Aside from the absence of dust structures in the images and the sense of the typical gradient (implying more extinction at larger radii), the gradients are so large that significant optical-band effects would be expected, since $A(4400\ \text{Å}) \sim 0.5A(1500\ \text{Å})$, where A is the total extinction in magnitudes. HUT spectroscopy also places strict limits on the amount of internal extinction (Ferguson & Davidsen 1993, Brown et al 1997). Instead, the gradients are apparently driven by a radial change in the properties of the old star population.

5. SPECTRAL AND PHOTOMETRIC CHARACTERISTICS OF THE UVX

5.1 Incidence, Spectral Shape, and Line Features

Except in cases of obscuration by a major dust lane (e.g. in edge-on S0-Sb objects), far-UV radiation has been detected in all nearby early-type systems observed with adequate S/N. As noted above (Section 3), this implies the presence of sources with $T_e > 8500$ K. Rifatto and colleagues (1995a, 1995b) have compiled all UV observations of galaxies published before 1990 and attempted to place them on a homogeneous system, which is a challenge owing to the varied types of experiments involved and the relatively low photometric precision which is typical. Their list includes 94 galaxies of type Sb or earlier with UV detections at $\lambda < 2100$ Å. The list does not include later photometry or imaging from the SCAP/FOCA balloon experiments (Milliard et al 1992, Donas et al 1995, Treyer et al 1998), *Atlas*/FAUST (Deharveng et al 1994), *Astro*/UIT (Stecher et al 1997), *Astro*/HUT (Kruk et al 1995), or the Maoz et al (1996) HST/FOC nuclear survey. Combined, these roughly double the total number of far-UV E-Sb detections, and HST is continually enlarging this sample. It is worth emphasizing that extragalactic UV observations are largely confined to relatively nearby, bright systems (except for very distant objects where the redshift brings the restframe UV into the bands accessible from the ground).

The early IUE spectra of the nuclei of bright ellipticals and spiral bulges (Johnson 1979, Bertola et al 1980, Perola & Tarenghi 1980, Nørgaard-Nielsen & Kjærgaard 1981, Oke et al 1981, Bertola et al 1982, Deharveng et al 1982, O'Connell et al 1986) showed immediately that the strong, broad emission lines characteristic of active nuclei were absent, excluding the AGN hypothesis. Signals for $\lambda \lesssim 2400$ Å were, however, very weak and subject to several kinds of detector noise (which generated some spurious claims of narrow coronal or chromospheric emission lines). Except in the brightest sources, it was necessary to average far-UV fluxes over bandwidths of $\sim$50 Å.

Burstein et al (1988, hereafter BBBFL) produced the largest homogeneous set of good IUE spectra for early-type galaxies (32 objects). Two examples are shown in Figure 4. The flux rapidly declines shortward of 3300 Å. Strong absorption features from Mg I (2852 Å), Mg II (doublet at 2800 Å), Fe I (numerous lines),

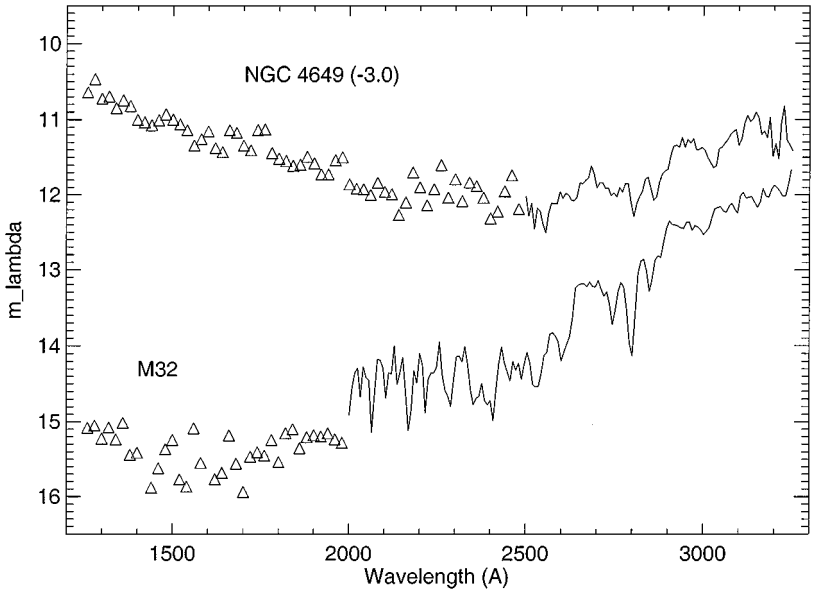

Figure 4 IUE spectra of two galaxies lying at the extremes of UVX behavior. M32 has the smallest known UV upturn, while NGC 4649 has one of the strongest. Data plotted with open triangles have 20 Å binning, while the solid line has 8 Å binning. The zero point of the NGC 4649 spectrum has been shifted −3.0 mags. Neither spectrum is corrected for redshift or foreground extinction. The FUV data for M32 are too poor to judge the slope of its UVX component. The weakness of the absorption lines near 2800 Å in NGC 4549 is caused by filling by the smooth UVX component, which contributes over 70% of the light at 2700 Å in this object. Reprocessed and recalibrated IUE spectra courtesy of RC Bohlin.

and other metallic species are easily detectable down to $\lambda \sim 2500$ Å, as are strong discontinuities caused by metallic blanketing at 2640 and 2900 Å. The mid-UV line spectrum closely resembles that of F-G dwarf stars (see Fanelli et al 1992), the spectral types expected for the main sequence turnoff in an old E-galaxy population. The flux reaches a minimum in the range 2000–2600 Å, where the S/N is almost always rather poor, then usually rises steeply again to shorter wavelengths. No maximum is detected in the rising component longward of the IUE cutoff at ∼1150 Å.

At the resolution permitted by the noise, the typical far-UV IUE spectrum is a relatively smooth continuum with an equivalent temperature $T_e \gtrsim 20000$ K. The spectral slope of the upturn is roughly constant, so that the far-UV rise begins at longer wavelengths in galaxies with brighter UVX components (e.g. NGC 4649 in Figure 4). The contribution of the UVX component to the mid-UV light can be appreciable, ranging up to 75% at 2700 Å for objects like NGC 4649 (BBBFL,

Ponder et al 1998, Dorman et al 1999), though this drops rapidly at longer wavelengths because of the steep rise in the spectrum of the cooler main sequence turnoff stars. In objects with the smallest UVX components (e.g. M32 and NGC 4382), the spectra appear to flatten below 2000 Å, rather than rise, but the S/N is too poor to estimate a temperature (BBBFL and Figure 4).

In the great majority of cases, E galaxy spectra longward of 3200 Å are quite similar to one another; the large spectral anomalies associated with the UVX are confined to the vacuum UV. This suggests that the stars responsible for the UVX are well segregated in the color-magnitude diagram from the bulk of the population. An interesting exception is M87, where anomalies are detectable up to 4000 Å (Bertola et al 1982, McNamara & O'Connell 1989); they are spatially extended and may be related to massive star formation in M87's cooling flow (see Section 8).

As originally emphasized by Tinsley (1972a), the characteristic FUV slope of UVX galaxies is consistent with star-forming models in which massive O and early B stars dominate the light. These require star formation to have occurred within the last 10–20 Myr. Tinsley did not discuss the far-UV spectral shape of her models, but later studies (e.g. Wu et al 1980, Gunn et al 1981, Nesci & Perola 1985, Rocca-Volmerange & Guiderdoni 1987, Bica & Alloin 1988, Burstein et al 1988, Ferguson et al 1991, Bruzual & Charlot 1993) would show that the young star and old, evolved star models could produce almost indistinguishable FUV energy distributions at low spectral resolution (see Figure 5). It would be necessary to consider other information, especially spectral features, to resolve the ambiguity.

Because of the limited signal-to-noise of individual spectra, IUE studies of possible far-UV absorption lines have been based on summed spectra for either the same or several objects. A serious complication is a systematic background of "fixed pattern" and camera artifact features in long-exposure IUE spectra (Crenshaw et al 1990). Welch (1982) analyzed 12 exposures of the center of M31 and detected weak absorption features at 1260 Å (Si II + S II), 1302 Å (O I + Si II + Si III), and 1335 Å (C II). The features were confirmed by BBBFL in M31, but they were weak or absent in a summed spectrum for 3 bright UVX E galaxies (BBBFL). These lines are characteristic of normal early-B stars (e.g. Fanelli et al 1992) but are considerably stronger in the stars than in any of the UVX sources. The strong Si IV (1400 Å) or C IV (1550 Å) absorption features associated with massive O stars were absent in both M31 and the summed E spectrum.

Welch (1982) and BBBFL argued that the weakness of the massive OB-star spectral features was inconsistent with recent star formation as the source of the UVX. BBBFL pointed out additional evidence in the form of continuum shapes. Although it is possible to produce a star-forming model whose spectrum matches the typical steep UVX far-UV spectral slope (see Figure 5), in fact many systems with younger populations (e.g. NGC 205 or 5102) have rather flat energy distributions in the 1200–3000 Å region. This is the signature of an aging starburst or a young starburst containing local extinction (Kinney et al 1993). Furthermore, the predicted young-star contamination of the optical band if the UVX originates in massive stars is significantly larger than limits from careful spectral synthesis

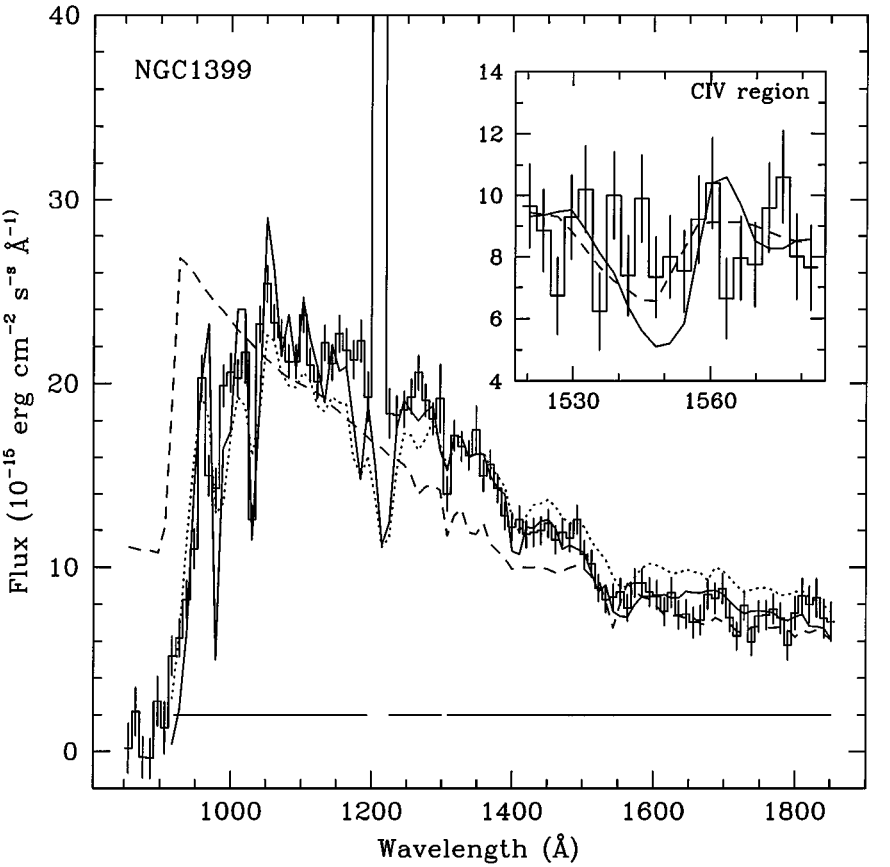

Figure 5 The *Astro*/HUT spectrum of the gE galaxy NGC 1399 in the Fornax Cluster (see Figure 2). The histogram is the observed flux in 10 Å bins. The solid line shows the best-fitting Kurucz (1991) solar abundance model atmosphere, which has T_e = 24000 K. The dashed line is a model from Rocca-Volmerange & Guiderdoni (1988) for an old galaxy with continuing star formation. This contains hotter starlight than is present in the galaxy. The inset shows the observed spectrum near the C IV 1550 Å doublet compared with continuous star forming models. From Ferguson et al (1991).

studies—e.g. the 2% maximum at 4000 Å set by Rose (1985) using high-resolution spectra of 12 E galaxies. The uniformity of the UV-upturn slope and the absence of warm-star effects at wavelengths longer than 2000 Å are therefore additional evidence against the involvement of massive stars in the UVX phenomenon.

The best far-UV spectra of UVX galaxies, covering the range 900–1800 Å, were obtained by *Astro*/HUT with a photon-counting detector and calibration superior to IUE's. HUT spectra of 8 early-type systems confirmed the weakness of the massive OB-star spectral features (Ferguson et al 1991, Davidsen & Ferguson

1992, Brown et al 1995, Brown et al 1997). For example, they placed an upper limit on the strength of C IV 1550 Å of $\lesssim$3 Å equivalent width in NGC 1399, which formally excluded spectral synthesis models for continuous star formation with normal metal abundances (see Figure 5). Equally important, by extending spectral coverage below 1150 Å, HUT was able to detect turnovers in the UVX spectra that place firm upper limits on their effective temperatures of $T_e \lesssim 25000$ K (equivalent to a B0 V star). This excludes continuing star formation models with a normal initial mass function (IMF). Only contrived models (e.g. invoking a truncated IMF or an unprecedented synchronization of star formation in different galaxies) can reconcile young populations with these results. The narrow T_e range, however, also appears to require an unusual degree of "fine-tuning" in an old population interpretation.

The HUT spectra also provide excellent limits on the amount of internal interstellar extinction. Because the slope of the far-UV spectral rise is nearly at the maximum encountered among hot stars (Dean & Bruhweiler 1985, Fanelli et al 1992), there is little room for interstellar reddening. In the HUT data, there is no evidence for extinction significantly in excess of the expected Galactic foreground. Since dust is normally associated with star-forming regions, this is yet further evidence of their unimportance in UVX galaxies.

The spectroscopic evidence therefore strongly corroborates the structural evidence from the last section that massive stars are not responsible for the UV-upturn.

Recently, Bica et al (1996) have produced composite spectra for groups of E galaxies from the IUE archives. They find evidence for broad absorption features at 1400 and 1600 Å in most UVX sources, which they identify with the Ly-α satellite lines in intermediate-temperature (DA5) white dwarf stars. If true, this would be remarkable since only a very unusual population would have the requisite concentration of white dwarfs. The features are not present in the better quality HUT spectra discussed above, but Bica et al suggest they are confined only to the nuclei and have been diluted by the larger HUT entrance aperture. This can be checked with HST/STIS.

5.2 Amplitude and Correlations with Other Properties

The most striking feature of the UVX phenomenon is its large variation from object to object. As measured by the color 1500–V, the amplitude of the UVX in the centers of bright E-Sb galaxies varies from $\sim$4.5 to $\sim$2.0, which is a factor of 10 in the ratio of far-UV to visible flux. No optical-IR photometric or spectral index for normal old stellar populations exhibits a comparable range; in fact, most do not vary more than $\pm$30% (e.g. Sandage & Visvanathan 1978, Peletier et al 1990, Trager et al 1998). The UV variations are not confined to the nuclear regions observed with IUE; they are also present in all the large aperture data sets cited above (OAO, ANS, UIT, HUT, FAUST, and the various rocket/balloon experiments).

Large excursions of this kind are usually associated with an incidental component rather than with the aggregate population of a galaxy. To what extent does the UVX convey useful information about the fundamental properties of galaxies?

A key insight was provided by Faber and her colleagues (Faber 1983, BBBFL): the UVX appears to be stronger in more metal-rich galaxies. Faber (1983) found in a small sample of early-type galaxies that nuclear UV colors became bluer as the nuclear spectral line index Mg_2, which measures the Mg I + MgH absorption features near 5170 Å, increased. The Mg features are produced by the dominant old stellar population, and this correlation simultaneously links the UVX to the bulk of the galaxy while further weakening the case for massive stars (since there is no obvious reason why recent star formation would be related to metal abundance). Interestingly, the correlation is reversed in sense from the well-known dependences of (U–B) or (B–V) colors on metal abundance in old populations. Driven mainly by opacity effects in stellar envelopes and atmospheres, these become redder as abundance increases.

The correlation was confirmed by the larger sample of BBBFL. They also found significant, if weaker, correlations between 1500–V and central velocity dispersion or luminosity. A later version of the Mg_2 correlation, including data on Galactic globular clusters, is shown in Figure 6. The figure emphasizes the lack

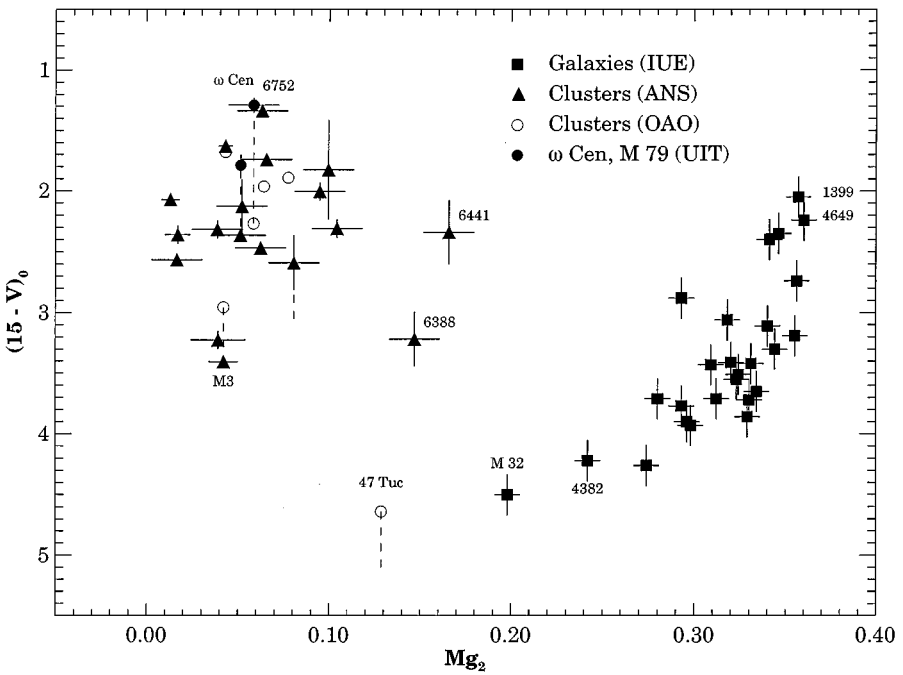

Figure 6 Amplitude of the UVX in old stellar populations, as measured by the color 1500–V, as a function of the Mg_2 line index, which measures absorption from Mg I + MgH near 5170 Å. The E galaxy data are from IUE, mostly from the study by BBBFL. The globular cluster data are from several sources, as indicated in the legend. The clusters and galaxies are clearly distinct kinds of populations. From Dorman et al (1995).

of continuity between the clusters and galaxies (see Section 6.1). Clusters with a wide range of Mg_2 index have large, if scattered, FUV fluxes. Some strong-lined clusters, e.g. 47 Tuc, are faint in the FUV while others, e.g. NGC 6388 and 6441, are bright. The galaxies with line strengths comparable to the strong-lined clusters are relatively faint in the FUV, but galaxy 1500–V colors rapidly become bluer as Mg_2 increases. The apparent correlation between 1500–V and Mg_2 is much stronger for the galaxies than the clusters. FUV behavior is only one of a number of basic spectrophotometric distinctions that show that globulars and E galaxies do not form a simple population continuum (e.g. Burstein et al 1984, Rose 1985, Ponder et al 1998).

Using the recent compilation of data for the Lick Observatory E galaxy spectral survey by Trager et al (1998), one can explore correlations between the UVX and other absorption line indices. There are good correlations, similar to that in Figure 6, between 1500–V and the Na I D lines or the CN bands at 4150 Å. But there is no correlation with a composite Fe index based on features at 5270 and 5335 Å. It is now clear that the abundances of certain light elements (N, Mg, Na) are decoupled from those of the iron peak in more luminous E galaxies (see reviews by McWilliam 1997 and Worthey 1998), although there is no clear understanding of the nucleosynthetic origin of these abundance ratio variations. The behavior of the UVX is evidently linked to that of the lighter elements.

The scatter in 1500–V at a given Mg_2 is appreciable, especially among the most metal-rich galaxies. This may indicate the influence of parameters other than metal abundance (see Section 6.3). It is also possible that the apparent correlation between UV colors and Mg_2 may not reflect smoothly varying properties but instead might arise from several discrete classes of galaxies, as discussed by DOR. There is a suggestion of grouping in Figure 6 (though this is less pronounced in the correlations with Na I and CN). Most of the galaxies have colors in the range 3.5 ± 0.5; within this group there is only a mild UV-Mg correlation. A few objects, including M32, have significantly redder colors. At the other extreme, there are four strong-lined objects with $1500\text{–V} < 3$ which stand out as a distinct group.

Interestingly, Longo et al (1989) have pointed out that the strongest UV upturns occur in objects with "boxy" isophotes. Most of the systems in the middle group of Figure 6 have "disky" isophotes. The isophotal distinctions between the two groups are now known to correlate with a wider set of morphological and kinematic properties (e.g. Jaffe et al 1994, Faber et al 1997). The boxy galaxies are probably merger products (Bender 1988). It is therefore possible that the UVX is influenced by the dynamical environment of galaxies. Alternatively, all of these characteristics may be related independently to the mass of galaxies.

In low resolution photometry of 40 early-type galaxies in the Virgo cluster, Smith and Cornett (1982) detected the effects of the long-wavelength tail of the UVX component in the integrated mid-UV colors (2400–V) of E galaxies. These, however, had a significantly different color-luminosity relation than the S0 galaxies in the sample. Such potential morphological dependencies have not been carefully investigated.

The UV-Mg_2-Na-N correlation and the large internal UV color gradients (Section 4.2) remain the most suggestive clues linking the UVX to the global properties of galaxies. Interpretations of the UVX must accommodate such correlations, but with the caveat that we do not yet really understand the nucleosynthetic drivers of E galaxy chemistry.

6. CANDIDATE LOW MASS UVX SOURCES

On the basis of the evidence in the last two sections, old, low-mass stars are the primary sources of far-UV light in E galaxies. Interpretational effort during the last 10 years has therefore focused on the viability of various types of hot, low-mass stars and their relationship to the dominant populations of E galaxies. Since observational information on the UVX is still sparse, much of this work has been based on new generations of theoretical models for advanced stellar evolution. A fully satisfactory interpretation has not emerged, but there has been good progress in narrowing the range of possibilities. In this section and the next we review the main conclusions.

6.1 Globular Cluster-Type Populations

The presence of hot stars in old populations was, of course, not unprecedented because "blue horizontal branch" (BHB) stars had long been associated with metal-poor globular clusters (having [Fe/H] $\lesssim -1$). The most natural old-star interpretation of the UVX was therefore that it arose from the low-metallicity tail of a stellar population with a large abundance range.

Surprisingly, however, observations quickly demonstrated that the UVX could not simply be the sum of globular cluster-type populations. The first quantitative comparison between clusters and a UVX source was made using ANS data for the bulge of M31 by Wu et al (1980). In order to fit the far-UV spectrum of M31, Wu et al were forced to add an additional high temperature component to the cluster M13, which has one of the hardest UV spectra among Galactic globulars. Models by Nesci & Perola (1985) likewise showed that normal cluster BHBs could not match the galaxy IUE spectra unless a second, hotter HB component was included. Oke et al (1981), Welch (1982), and Bohlin et al (1985) all emphasized the dissimilarity between typical cluster and galaxy UV energy distributions. Compilations of ANS, IUE, HUT, and UIT data for globulars (van Albada et al 1981, Castellani & Cassatella 1987, Bica & Alloin 1988, Davidsen & Ferguson 1992, Dorman et al 1995) show that although clusters in general have total UV-bright star fractions exceeding those of galaxies (see Figure 6), galaxies can have steeper far-UV spectra than any cluster. The distinction between the two populations is quite clear in two-color diagrams such as Figure 7, where the color 1500–2500 is used to measure the slope of the UV upturn.

The temperature distribution of UV-bright sources in the clusters is evidently cooler and broader than in the galaxies. The far-UV slope in the galaxies is

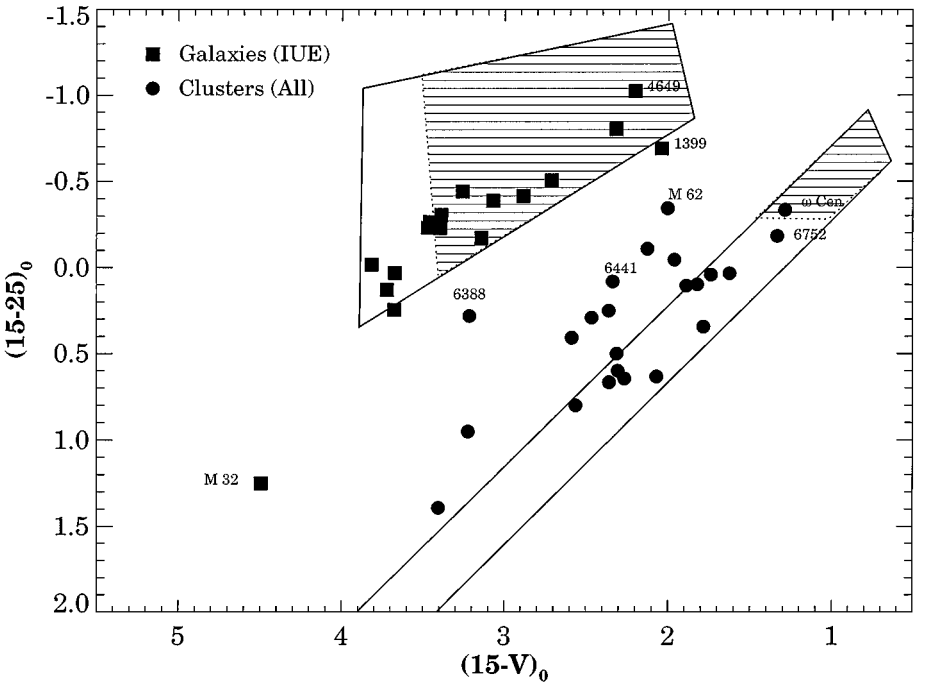

Figure 7 Broad-band UV colors for E galaxies and globular clusters compared. Data are mainly from IUE. The color 1500–2500 measures the slope of the UV-upturn component, while 1500–V measures its amplitude. Globular clusters and galaxies are clearly segregated in the diagram, with galaxies having steeper FUV spectral slopes at a given amplitude. The boxes enclose several fiducial model sets, with the upper one corresponding to $Z \gtrsim Z_\odot$ and the lower to $Z \lesssim 0.04\ Z_\odot$. The shaded regions represent models in which the hot stellar component consists mainly of EHB stars. Most of the galaxies require an EHB contribution, but most of the clusters do not. From Dorman et al (1995).

equivalent to $T_e \gtrsim 20000$ K, whereas BHBs in Galactic globulars normally do not extend beyond $T_e \sim 10000$–12000 K. Hotter stars can be found in some globulars on or above the horizontal branch, as Hills (1971) originally pointed out, but these are relatively uncommon (see de Boer 1985, 1987; and Section 6.2). Even where hotter stars are present, the mean integrated UV light of typical clusters is heavily influenced by cooler horizontal branch objects with a wide range of temperatures. Lower metallic line blanketing in the atmospheres of cluster stars on the warm HB and near the main sequence turnoff also produces larger mid- and near-UV emergent flux than for galaxies, tending to flatten the UV energy distributions.

Even if one ignores the distinctions between clusters and galaxies in UV spectral shape, the limits on metal-poor light at optical wavelengths in M31 and E galaxies are inconsistent with a large contribution from cluster-like populations

in the UV (O'Connell 1976, 1980; Rose 1985; Bica & Alloin 1988; Dorman et al 1995).

The fact that the galaxy UVX does not appear to arise from a metal-poor subpopulation similar to the Galactic globular clusters does not, of course, necessarily mean that the kinds of hot stars in the galaxies differ from those in the clusters—only that the mixture of these is different.

6.2 Single Star Candidates

Since there were no ready-made local analogues for UVX populations, it was necessary to explore alternatives from a largely theoretical perspective. The seminal discussion of the various low-mass candidates for the UVX sources was presented by Greggio & Renzini (1990, hereafter GR; an updated overview is in Greggio & Renzini 1999). They discussed primarily single-star candidates, since the parameter space for binaries is much larger. Here, we also defer discussion of the possible involvement of binaries until a later section.

On the basis of the UV/optical colors, the UVX is estimated to contribute ~2–3% of the bolometric luminosity in the most metal rich galaxies such as NGC 1399 and 4649 (GR). While this is not large, the challenge is to identify a mechanism for producing sufficient numbers of high-temperature stars in old populations. If the relevant evolutionary phase is short-lived compared with the lifetime of the galaxy, then the number of stars in this phase is proportional to its evolutionary lifetime. In this circumstance, the "fuel consumption theorem" shows that its contribution to the bolometric luminosity of the galaxy is proportional to the total amount of nuclear fuel consumed during the phase, which can be estimated directly from interiors models (Tinsley 1980, Renzini 1981a, Renzini & Buzzoni 1986, GR). Interesting candidates for the UVX will therefore have temperatures over ~20000 K and will burn up to ~0.01 $M_\odot$ of hydrogen or ~0.1 $M_\odot$ of helium (GR). Dorman et al (1995, hereafter DOR) used a similar approach to estimate that the integrated monochromatic energy release at 1500 Å of suitable candidate evolutionary phases must be $E_{1500} \gtrsim 4 \times 10^{-3}\ L_{V,\odot}$ Gyr Å^{-1}, where $L_{V,\odot} = 4.51 \times 10^{32}$ ergs s^{-1}.

The evolutionary phases of interest all occur after a low-mass star has begun moving up the red giant branch. HR diagram loci for the main types of UVX candidates that have been explored to date are illustrated in Figure 8. The general considerations are described in GR. The evolutionary trajectory of a low-mass star following He core ignition at the tip of the red giant branch is governed mainly by its envelope mass, M_{ENV}. Since the He core mass is ~0.5 $M_\odot$ and is relatively insensitive to other parameters, $M_{ENV} \sim M_{TO} - \Delta M - 0.5\ M_\odot$, where M_{TO} is the turnoff mass and ΔM is the total mass loss during the red giant phase, which, in globular cluster stars, amounts to ~0.1–0.3 $M_\odot$, or 10–40% of the initial mass. The variance in mass loss leads to a scatter in M_{ENV} and hence in the initial temperature of the subsequent core He-burning stage on the "zero-age" horizontal branch (ZAHB). Envelope masses on the HB range up to ~0.4 $M_\odot$. The lower

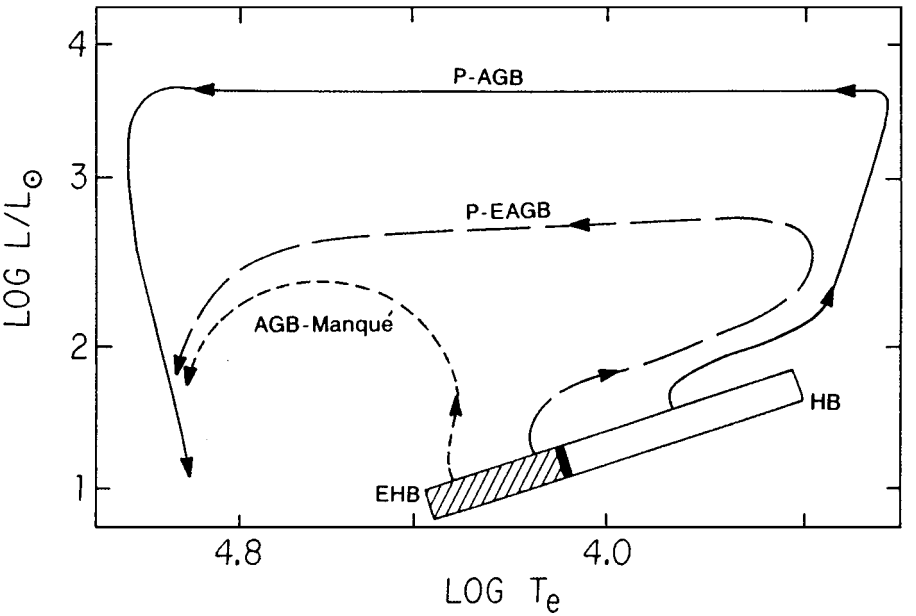

Figure 8 Schematic evolutionary tracks for the principal post-horizontal branch evolutionary phases described in Section 6. Envelope masses on the horizontal branch increase from left to right. For $Z \sim Z_{\odot}$, they are $M_{ENV} \sim 0.003$ $M_{\odot}$ at the left hand (hot) edge and $\sim$0.05 $M_{\odot}$ at the heavy separator line, which marks the cool end of the "extreme horizontal branch" (shaded). The segment of the "P-AGB" track (solid line) which rises to the right of $\log T_e \sim 3.6$ corresponds to the AGB. Detailed evolutionary tracks for these phases are shown, for example, by Dorman et al (1993).

is M_{ENV}, the hotter is the ZAHB location (e.g. Iben & Rood 1970, Rood 1973, Sweigart 1987, Dorman 1992). Envelopes smaller than 0.05 $M_{\odot}$ correspond to T_e(ZAHB) $\gtrsim$ 14000 K. After $\sim$100 Myr, helium becomes exhausted in the center of the star, which then contains both helium-burning and hydrogen-burning shells moving outward.

If M_{ENV} is large enough, post-HB stars develop a deep convective envelope, evolve to lower temperatures, and ascend the cool asymptotic giant branch (AGB), leaving it only at high luminosity near the AGB tip, when rapid mass loss and thermal shell pulsing remove the envelope. Subsequent evolution in this case involves a rapid (10^4–10^5 yr) contraction and heating (the post-AGB or PAGB phase), in some cases with the formation of a planetary nebula, followed by cooling and fading on the white dwarf remnant sequence. Much of the pre-white dwarf time is spent at high temperatures, $T_e > 50000$ K. PAGB models for low-mass stars have been computed by Schönberner (1983), Blöcker & Schönberner (1990), and Vassiliadis & Wood (1994). The great majority of stars now near or above the main sequence turnoff in globular clusters will pass through the PAGB channel.

More exotic evolution can occur in the case of very small envelopes. For $M_{ENV} \lesssim 0.05$ $M_\odot$ the post-HB star may evolve to higher temperatures before it reaches the AGB tip or even before it approaches the cool AGB. These cases produce, respectively, post-early AGB (PEAGB) and AGB-manqué ("failed AGB") stars (see Figure 8). The first detailed models were described by Brocato et al (1990) and Caloi (1989), respectively (though similar behavior had been noted in early models by Sweigart et al 1974 and Gingold 1976). Their internal structure is similar to that of an AGB star (a double shell source) but with much thinner envelopes. They burn about the same amount of fuel as do the more familiar cool AGB stars, but they do so at much higher T_e ($\sim$25000 K). Their post-HB paths in the HR diagram can be convoluted. AGB-manqué lifetimes are $\sim 10^7$ yr, considerably longer than for the PAGB phase, after which stars evolve directly to the remnant cooling sequence. Typical E_{1500}'s for these "slow blue" post-HB phases (Horch et al 1992) are comparable to those of the hot HB phase (DOR Figure 6). Grids of such models, for a wide range of metallicities, have been computed by Castellani & Tornambè (1991), Castellani et al (1992), Horch et al (1992), Dorman et al (1993), Bertelli et al (1994), Castellani et al (1994), and Yi et al (1997a).

The least massive envelope ($\sim$0.05 $M_\odot$, if $Y \sim Y_\odot$; see Dorman et al 1993, Table 1) capable of producing a classical PAGB star yields a boundary on the ZAHB between what is now called the "extreme HB" (EHB) (to higher temperatures) and the normal HB. This is marked on Figure 8. AGB-manqué progenitors occupy the hot end of the EHB, while PEAGB progenitors occupy the end adjacent to the normal HB. Note that the normal main sequence for massive stars (not shown) crosses the HB locus at $T_e \sim 10000$ K, and that HB objects hotter than this fall below the main sequence in the classical "hot subdwarf" regime.

Another variety of hot star can be produced directly from the first ascent red giant branch if mass loss is large enough to remove the convective envelope before core He ignition. In this case, the post-RGB (PRGB) object evolves rapidly to the white-dwarf cooling sequence without passing through the HB phase. Some such objects may experience a late He-flash while on the cooling sequence as their central temperatures rise owing to gravitational core contraction. These "hot flashers" will then move to a position slightly below the EHB and follow subsequent post-EHB tracks similar to normal EHB stars. The hot flash effect was demonstrated by Castellani & Castellani (1993), and more detailed models including the secular effects of mass loss during advanced RGB evolution have been computed by D'Cruz et al (1996).

Remnants on the white dwarf cooling sequence are the inevitable descendants of all the preceding types of stars. During their early evolution, white dwarfs are still hot enough to emit UV photons, and their potential contribution to galaxy light can be estimated by integrating down the cooling curve. Magris & Bruzual (1993) and Landsman et al (1998) find that hot white dwarfs (residing on the cooling curve for $\lesssim$200 Myr) can contribute up to $\sim$10% of the far-UV light produced by their parent PAGB phases (less if their parents were EHB stars). This is too small to be of practical importance in normal circumstances. Unless one invokes an IMF

truncated below $\sim$1.5 $M_\odot$, the integrated spectrum of the cooling curve also does not contain the strong Ly-α satellite features claimed by Bica et al (1996) to be present in IUE spectra of galaxies.

Finally, the much-studied "blue stragglers" (Bailyn 1995), which are warm stars lying near the main sequence but above the turnoff luminosity in star clusters, are too cool to be viable UVX candidates. They generally have temperatures below 10000 K. However, they may influence the mid-UV spectrum of old populations (Spinrad et al 1997, Landsman et al 1998).

A common characteristic of the viable UVX candidates is their extreme sensitivity to small changes in properties. Differences of only a few 0.01 $M_\odot$ in envelope mass for hot HB stars produce large changes in the type of post-HB track followed and the resulting E_{1500} (e.g. see DOR Figure 6). Likewise, models for PAGB stars show that their UV output is extraordinarily sensitive to core mass. Schönberner's (1983) 0.546 $M_\odot$ model has a lifetime 20$\times$ longer than for his 0.565 $M_\odot$ model and has E_{1500} a factor of 6.8 larger (DOR; GR Figure 3).

Likely individual examples of all these candidate types have been found in local star clusters and the Galactic field. Imaging with space telescopes has produced a fairly large sample of PAGB, EHB, AGB-manqué, and related post-HB stars in some globular clusters (e.g. in ω Cen, Whitney et al 1994, 1998; NGC 6752, Landsman et al 1996; NGC 2808, Sosin et al 1997; NGC 6338 and 6441, Rich et al 1997; M13 and M80, Ferraro et al 1998). A smaller sample of similar sources has been identified in the open clusters NGC 188 and 6791 (Liebert et al 1994, Landsman et al 1998), and Landsman et al estimate that NGC 188 and 6791 would have UV upturns in their integrated light as strong as any E galaxy. Over 1500 hot subdwarfs (sdO, sdB, and related types) are now known in the Galactic field. As first shown by Greenstein & Sargent (1974), many of these are EHB and post-EHB stars (Heber 1992, Saffer et al 1994). Kinematical studies show that some hot subdwarfs are members of the old, metal-rich disk population of the Galaxy (Thejll et al 1997). The field and open cluster examples are important cases since they demonstrate that EHB objects are not confined to low-metallicity environments. NGC 6791, in particular, has [Fe/H] $\sim +0.5$ (Kaluzny & Rucinski 1995).

DOR summarized integrated UV outputs for the several main candidate UVX star types. PAGB tracks have $E_{1500} < 0.001\ L_{V,\odot}$ Gyr Å^{-1}. They therefore cannot be solely responsible for the brightest UV-upturn cases, as first pointed out by GR and Castellani & Tornambè (1991). However, the EHB, PEAGB, and AGB-manqué phases burn more H + He fuel at high T_e's, by factors of $\sim$3–30, than classical PAGB stars and therefore are excellent UVX candidates.

6.3 Relationship to Global Characteristics of Parent Population

Each UVX candidate represents a potential channel to be filled by its evolving post-main sequence parent population. At least five global population parameters are known to be important in determining the occupation of the various channels.

The effects of these have been reviewed in GR and Chiosi (1996). Yi et al (1997b) nicely illustrate the effects of age, abundance, and mass-loss parameters on color-magnitude diagrams, integrated spectra, and broad-band UV colors. The single most important variable is mass loss on the giant branch, followed by helium abundance (Y).

Age As a population ages, its turnoff mass decreases, with $M_{TO} \sim 0.96\, t_{10}^{-0.2}\, M_\odot$, where t_{10} is the age in units of 10 Gyr. For a given amount of RGB mass loss, older stars will have smaller M_{ENV} and will fall at higher ZAHB temperatures. The UVX is therefore expected to increase with age, though probably in a strongly nonlinear fashion. At large enough ages, all stars evolving up the RGB will become hot EHB or PRGB objects.

Y An increase in helium abundance has important effects on post-giant branch evolution (GR, Horch et al 1992, DOR). Because of the increase in mean molecular weight, turnoff masses at a given age are smaller, which yields smaller M_{ENV} for a given amount of RGB mass loss. A higher initial helium abundance also causes stars with a given M_{ENV} to burn more of their hydrogen envelope during the core He-burning phase, producing AGB-manqué behavior for a larger range of M_{ENV}'s (Horch et al Table 1; DOR Figure 6). Increasing Y from 0.27 to 0.47 roughly quadruples the total E_{1500} for a uniform distribution of M_{ENV}'s (DOR).

Z The strong correlation between the UVX and line strengths discussed in Section 5.2 makes metal abundance effects on hot star evolution of particular interest. Based on the example of the globular clusters, one might suppose that metal abundance determines the prevalence of hot HB stars. To the contrary, theoretical models show that Z has little direct effect on either the EHB or post-EHB phases of evolution (e.g. Dorman et al 1993, DOR). Instead, these are governed mainly by M_{ENV}. Although increased metallicity does increase M_{TO} for a given age, thereby decreasing ZAHB temperatures for a given amount of RGB mass loss, hot HB stars can appear at any metal abundance as long as envelope masses are small enough. This is demonstrated in the grids of metal-rich HB models cited in Section 6.2 and was first illustrated in integrated light by Ciardullo & Demarque (1978). However, for higher metallicities, T_e for medium-envelope (0.05–0.15 $M_\odot$) stars is strongly decreased. This implies that a uniform distribution of M_{ENV} will lead to a bimodal distribution of ZAHB temperatures at higher metallicities (Dorman et al 1993, D'Cruz et al 1996).

There has been less exploration of advanced evolution with relative abundance variations among the metals. D'Cruz et al (1996) found no qualitative changes in behavior for models with [O/Fe] $= +0.75$. However, as discussed in Section 5.2, models incorporating variable abundance ratios among the metals would seem to be essential if the empirical line strength correlations are to be understood.

These theoretical expectations on the secondary status of metallicity effects on HB temperatures have good empirical support. The bluest UV colors in Figure 6

occur not for the most metal-poor globular clusters but for those of intermediate metallicity. Small numbers of EHB and related stars have recently been found in globular clusters with heavily populated red HBs (NGC 362, Dorman et al 1997; 47 Tucanæ, O'Connell et al 1997), and large numbers of hot HB stars are present in the relatively metal-rich clusters NGC 6388 and 6441 (with $Z \sim 0.25\ Z_\odot$, Rich et al 1997). Other clusters with EHB stars may range up to $Z \sim 3\ Z_\odot$ (NGC 6791, Liebert et al 1994).

$\Delta Y/\Delta Z$ There is good evidence from the study of emission lines in low-metallicity galaxies that helium abundance is coupled to metal abundance (e.g. Wilson & Rood 1994, Izotov & Thuan 1998). Values of $\Delta Y/\Delta Z \sim 3$–4 have been derived for low metallicity environments. If these apply to E galaxies, then the smaller effects on EHB and post-HB evolution of metallicity enhancements for $Z \gtrsim Z_\odot$ are strongly amplified by the effects of Y enhancement, as emphasized by GR. The dramatic increases in post-HB UV output found by Horch et al (1992) in metal-rich models were actually produced by the accompanying He effects (Y is increased to $\sim$0.35–0.45 for $Z > 2\ Z_\odot$ in their models). Jørgensen & Thejll (1993) estimated that $\Delta Y/\Delta Z > 2.5$ is needed to produce a strong positive correlation between metal abundance and UVX above $Z_\odot$, for normal ranges of age and RGB mass loss. DOR (Section 8.3) emphasize that there is very little known about $\Delta Y/\Delta Z$ for solar abundances or above and that most available chemical evolution models suggest smaller He enhancements than for low abundances. DOR also point out that EHB stars exist in clusters and the Galactic field at moderate metallicites, and presumably moderate Ys, so that extreme Z or Y enhancements are not essential to their production.

Mass Loss Mass loss is the most important determinant of post-RGB evolution in low-mass stars but is also the most difficult to evaluate because of a paucity of both empirical evidence and theoretical exploration. RGB mass loss is usually modeled using the Reimers (1977) prescription:

$$\dot{m} = -4 \times 10^{-13}\ \eta_R\ \frac{L}{gR}\ M_\odot\ \mathrm{yr}^{-1},$$

where η_R is a mass loss efficiency parameter, L is the luminosity, g is the surface gravity, and R is the radius, with $L, g,$ and R in solar units. This formula is based on dimensional analysis rather than a well-grounded physical theory. It is consistent with the available observational data, which indicate only that mass loss increases with luminosity and decreasing surface temperature, reaching a maximum just prior to the He flash (reviewed in Dupree 1986). The Reimers prescription implicitly includes composition and age dependences through their influence on stellar structure, and hence $L, g,$ and R. Although η_R is the principal mass-loss parameter in this formulation, empirically there is always a significant spread in the effective η_R (e.g. Rood 1973), which produces a range ΔM_{ENV} on

the ZAHB. There is no theory for the spread at the moment, so it appears in evolutionary synthesis models as an additional free parameter.

To produce a typical globular cluster blue horizontal branch requires $\eta_R \sim 0.2$–0.5 (e.g. Renzini 1981b, Yi et al 1997b) if cluster ages are $\sim$15 Gyr. Such values are therefore regarded as "normal" and are widely used in galaxy spectral modeling. However, the globular cluster values would increase if the lower ages of $\sim$12 Gyr favored by the recent Hipparchos recalibration of distance indicators are adopted (Yi et al 1999). Furthermore, there is very little evidence on whether globular cluster η_R values are appropriate in other kinds of stellar populations. It is physically plausible that η_R would increase with metal abundance, owing to grain formation, for instance. GR explored the consequences of assuming that $\eta_R \propto 1 + \frac{Z}{Z_{crit}}$, where Z_{crit} is a critical threshold. D'Cruz et al (1996) and Yi et al (1997b) considered models for a range of η_R up to 1.2, the former including self-consistently the effects of mass loss on evolution near the RGB tip and the "hot flasher" phenomenon. They find that production of EHB stars in populations with $Z \gtrsim Z_\odot$ requires $\eta_R \gtrsim 0.7$, with total mass loss of $\sim$0.5 $M_\odot$ per star for ages $\gtrsim$10 Gyr. D'Cruz et al found that a smooth distribution of η_R on the RGB leads to a strongly bimodal distribution of ZAHB temperatures if $Z \gtrsim Z_\odot$. The models imply that increases of η_R of only a factor of 2–3 over canonical globular cluster values are sufficient to produce a large population of EHB and post-EHB stars for normal ranges of age, Z, and Y.

The hot flash phenomenon is one way of routing a significant fraction of the evolving population into HB objects with $M_{ENV} < 0.05$ $M_\odot$ without the need for "fine tuning" of mass loss. D'Cruz et al (1996) showed that as long as mass loss near the RGB He flash luminosity is above a critical threshold (corresponding to $\eta_R \sim 0.7$, but not necessarily tied to the Reimers prescription), EHB stars will always be produced via the hot-flash mechanism. Neither the η_R values nor the range of values ($\Delta\eta_R$) producing EHB objects vary much with metallicity from globular cluster to supersolar values. The mechanism produces a natural concentration to a narrow range of T_e. There is also improving empirical evidence from the cluster and field samples (Section 6.2) that EHB populations do occur in nature at a wide range of metallicities. Thus, there are no obvious obstacles to the production of EHB stars through enhanced mass loss.

Although the Reimers law provides a useful schematic for exploring mass-loss effects on the UVX, a much improved physical theory is needed. Preliminary hydrodynamic models (e.g. Bowen & Willson 1991, Willson et al 1996) suggest a sudden onset of mass loss at a critical luminosity and a strong metallicity dependence, effects that may not be well modeled by a simple scaling law.

Other Parameters There are certainly other processes that can influence the production of hot stars in old populations. Sweigart (1997) showed that deep mixing in the outer envelopes of RGB stars, which results in enhanced surface He abundances, encourages the production of hot HB stars and AGB-manqué behavior. Larger mixing is presumably related to higher stellar rotation rates. The dynamical environment of galaxies could therefore influence the UVX by way

of stellar spin distributions. Ferraro et al (1998) find that gaps in the hot HBs of different globular clusters occur at similar temperatures, suggesting that RGB mass loss is a multimode process. Good candidate mechanisms have not yet been identified.

6.4 Binaries and Dynamical Effects

There has been much speculation about the possible origin of hot low-mass stars through dynamical interactions, especially in binary systems through Roche-lobe mass transfer or mergers. The various recognized mechanisms have been reviewed by Bailyn (1995), while their implications for the UVX problem were most extensively discussed by GR. The mildest form of interaction occurs when a star ascending the giant branch loses part of its expanding envelope to a companion, thereby appearing with lower M_{ENV} on the ZAHB (Mengel et al 1976) but evolving normally thereafter. Based on the frequency of binaries among the sdB stars in the Galactic field (Green 1999), this process may be fairly common there. Although "fine tuning" of binary mass ratios and separations would seem to be necessary to produce small M_{ENV} without suppressing the He flash altogether, in fact the hot-flash mechanism (D'Cruz et al 1996) would mitigate this problem here as it does for normal mass loss. One reason that UV star production in binaries might depend on Z is that stellar envelopes become more inflated at higher metallicities (GR). The fact that field and cluster hot horizontal branches have gravities and luminosities consistent with single-star models suggests that more drastic interactions (e.g. mergers) are considerably more rare.

Some support for dynamical effects is provided by the observation that the extent of horizontal branch "blue tails" in Galactic globular clusters appears to correlate with cluster concentration and density (e.g. Fusi Pecci et al 1993, Buonanno et al 1997). However, other expectations for dynamical mechanisms are not met. For instance, the hot stars are not necessarily concentrated to the centers of clusters, and the system with the largest EHB/post-EHB population (ω Cen) is notably low density (e.g. Whitney et al 1994, Rich et al 1997). HST observations of 10 cluster cores (Sosin et al 1997) show that the EHB stars are not as centrally concentrated as the blue stragglers (which are almost universally agreed to be interaction products).

It is unclear how to translate the evidence for dynamical mechanisms in star clusters to the dynamical environment of galaxies, which is very different and less conducive to stellar interactions. Of course, the present field population in E galaxies may well have originated in concentrated cluster-like systems that have since disintegrated but which were responsible for establishing the binary frequency. Stellar rotation, which could depend on global dynamical characteristics of galaxies, may also influence the UVX through He mixing (Sweigart 1997). The only hint that the E galaxy UVX is related to dynamics is the connection between large UV upturns and boxy isophotes (Longo et al 1989 and Section 5.2). The core of M32 is the densest observable extragalactic system. No large radial gradients in blue light are apparent near its center at HST resolution (King et al 1992, 1995;

Bertola et al 1995; Cole et al 1998; Lauer et al 1998), though Brown et al (1998a) note that the density of resolved UV stars per unit total light increases slightly at smaller radii in both M31 and M32.

Mass transfer onto white dwarf binary companions can produce copious UV flux and has also been discussed in the context of the UVX by GR. One of the main problems is again the fine-tuning needed to ensure a sufficient but not excessive transfer. Because of the large parameter space involved, estimates are only tentative, but accreting white dwarfs seem unlikely to be major contributors to the UVX (GR). The UV spectrum of a population dominated by such objects is also expected to show fairly strong emission lines (e.g. Wu et al 1992), which are absent in E galaxy spectra.

Although dynamical interactions could certainly influence the UVX in galaxies, there is no strong evidence yet that they do so.

7. HOT LOW-MASS STARS IN ELLIPTICAL GALAXIES

7.1 Interpretation of UV Spectra and Colors

Early discussions of low-mass candidates for the UVX in the context of the observations concentrated mainly on distinguishing them from the massive star interpretation rather than from one another. Rose & Tinsley (1974) were the first to emphasize that hot PAGB stars were inevitable products of low-mass evolution and should be present in sufficient numbers to affect the integrated UV spectrum in old populations of all metallicities (assuming mass loss is not so extreme as to suppress the AGB phase altogether). O'Connell (1976) found tentative evidence for hot starlight in the 3300–4000 Å region of 3 gE galaxies, which was plausibly interpreted as from the PAGB. Following the demonstration that normal HB stars in globular cluster-like populations were not compatible with the galaxy UVX spectra (see Section 6.1), PAGB stars became the favored candidates.

Bohlin et al (1985), Renzini & Buzzoni (1986), and O'Connell et al (1986) pointed out that the extreme sensitivity of the UV output of PAGB stars to their core masses might explain the large variation in UVX strength and the Faber (1983) Mg_2 correlation. They suggested that metallicity-enhanced mass loss or age differentials drove the correlation. BBBFL, Bertelli et al (1989), and Magris & Bruzual (1993) examined the implications of PAGB models quantitatively. They found that the brightest UVX sources would require non-PAGB sources of UV light or PAGB stars with core masses smaller than those in the grid of evolutionary models by Schönberner (1983), the smallest of which was technically a PEAGB rather than a PAGB star (i.e. it did not reach the AGB tip). They also concluded that changes in Z alone could not reproduce the Faber correlation unless there were accompanying changes in t, η_R, or Y.

Shortly thereafter, two lines of evidence combined to reject PAGB stars as the principal UVX sources. First, GR and the other studies cited in Section 6.2 emphasized the shortfall in the UV output of PAGB objects compared with the

strongest upturn galaxies and suggested EHB stars and their descendants as a more viable alternative. Second, HUT spectroscopy showed that the energy distributions of M31 and NGC 1399 declined shortward of 1050 Å (Ferguson et al 1991, Ferguson & Davidsen 1993). This placed an upper limit of $T_e \sim 25000$ K on the temperature of the dominant UVX stars, considerably cooler than the 50000 K characteristic of a PAGB component but entirely consistent with the EHB and post-EHB channels. Ferguson & Davidsen (1993) found significant differences between M31 and NGC 1399 which demonstrated, independent of modeling details, that the UVX is probably a composite population with the mixture of HB and other hot types varying from system to system. (Later HUT observations by Brown et al 1997 confirmed such variations in six other galaxies based on 912–1000 Å fluxes.)

EHB, PEAGB, and AGB-manqué stars have consequently become the favored candidates for the dominant UVX sources. They are energetically viable since in the brightest UVX cases only 10–20% of the evolving stars in the dominant population would need to pass through the EHB and post-EHB channels to produce the observed far-UV luminosities (GR, DOR, Brown et al 1995). DOR showed that the observed 1500–V and 2500–V colors of E galaxies were consistent with composite EHB/post-EHB and PAGB models in which the EHB channel contributes ∼25% of the FUV light in medium-upturn systems like M31 but ∼75% in the strongest upturns. They found that most globular clusters do not require EHB stars to explain their UV colors, consistent with independent information on color-magnitude diagrams (see Figure 7). They also found that if mass loss is left as a free parameter, 1500–V does not place useful limits on galaxy age or metal abundance, though 2500–V does. This is because the properties of the EHB/post-EHB channels are not very sensitive directly to either parameter, whereas the main sequence turnoff (which dominates for $\lambda > 2500$ Å) is. DOR found acceptable agreement with observed colors for a wide range of ages (6–20 Gyr) but only for solar or higher metallicities ($Z \sim 1$–$4\ Z_\odot$), again leaving mass loss unconstrained.

Brown et al (1997) analyzed HUT spectra of six E/S0 galaxies covering the 900–1800 Å region at 3 Å resolution. They were able to produce good fits to the spectra with composite EHB/post-EHB and PAGB models in which only a small fraction ($\lesssim$10%) of the evolving population need pass through the EHB channel (see Figure 9). Although the models formally contained very small ranges of M_{ENV} on the ZAHB (e.g. 0.021–0.046 $M_\odot$ in NGC 4649), they found that broader distributions of M_{ENV} would yield similar fits because the short wavelength FUV flux tends to be dominated by the hot AGB-manqué phases. The best fits occur for evolutionary tracks with supersolar values of Z (2–3 $Z_\odot$) and Y (0.34–0.45), which produce more flux than subsolar models below 1200Å. Interestingly, however, fits are better for atmospheres with subsolar values of Z (∼0.1 $Z_\odot$). Brown and colleagues attribute this to the same processes (mainly diffusion) that create well-known abundance anomalies among Galactic hot subdwarfs (e.g. Saffer & Liebert 1995). These effects are not straightforward to analyze, but the expectation is that diffusion in high-abundance stars will tend to reduce line strengths and make

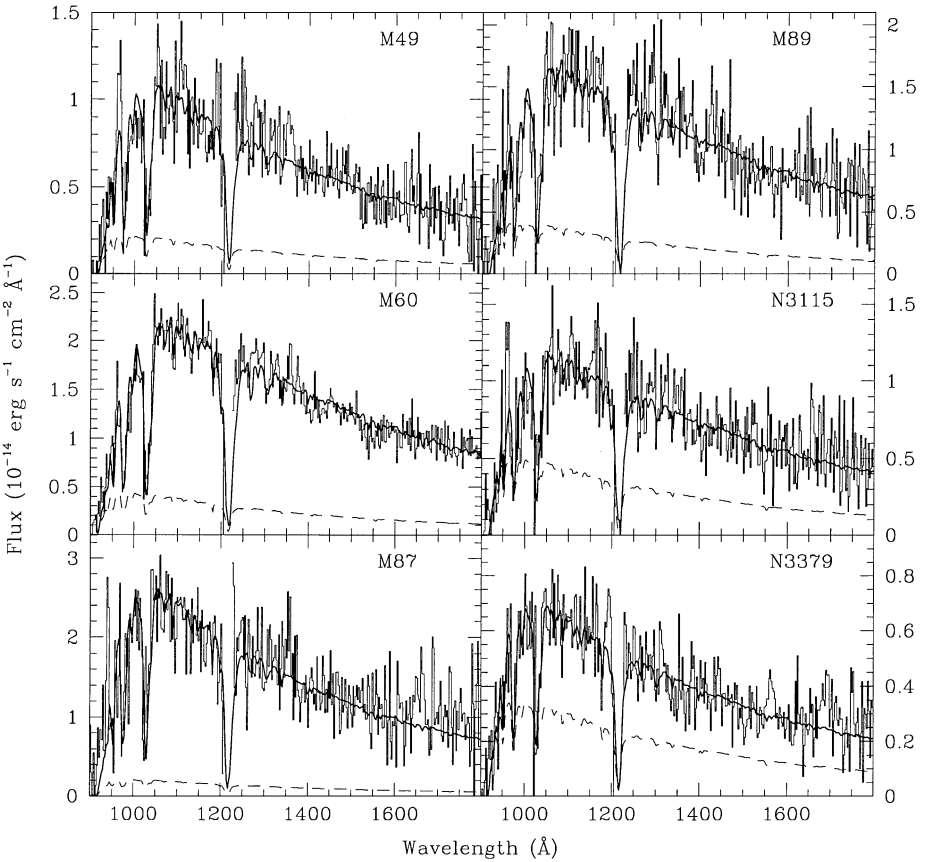

Figure 9 *Astro*/HUT far-UV spectra of 6 E/S0 galaxies compared with EHB+post-EHB+PAGB models. Fluxes are shown in 2.5 Å bins. The best-fitting composite models are shown by the solid lines. These employ evolutionary tracks with $Z \sim 2$–$3\ Z_{\odot}$ but atmospheres with $Z = 0.1\ Z_{\odot}$. The PAGB contribution to each model is shown by the dashed lines; this is usually considerably smaller than 50%. From Brown et al (1997).

spectra appear less metal-rich. This is a critical issue, however, since the consensus interpretation would have to be fundamentally revised if the UVX arose from a metal-poor population.

The DOR and Brown et al (1997) analyses were consistent with realistic global population models but left mass loss on the RGB as a free parameter because the physics involved are so uncertain. A large body of other evolutionary spectral synthesis studies adopt definite prescriptions for mass loss and have predicted the UV spectra of old populations with the intent of exploring how higher metal abundances might produce larger UV output (as in Figure 6). Some of these consider a fixed grid of abundance parameters, while others (e.g. the Padova group, Bressan

et al 1994, 1996) include self-consistent star formation and nucleosynthetic enrichment histories to determine the abundance distribution in galaxy models of various masses. In most of these models, RGB mass loss is specified by the Reimers prescription using a fixed mean η_R value in the range $\sim$0.3–0.5, as appropriate for globular clusters (e.g. Bertelli et al 1989, Barbaro & Olivi 1989, Bruzual & Charlot 1993, Magris & Bruzual 1993, Bressan et al 1994, Lee 1994, Bertola et al 1995, Bressan et al 1996, Chiosi et al 1997, Park & Lee 1997). These model sets do not include the "hot flash" phase. It is also necessary to specify the spread of M_{ENV} on the ZAHB, ΔM_{ENV}. Since the early studies of globular cluster HBs (e.g. Rood 1973) it has been traditional to use a modified Gaussian distribution, though this is neither unique nor well justified on astrophysical grounds.

The two-color diagram in Figure 10 (from Yi et al 1997b) illustrates the general nature of the predictions from this class of models. It shows the effects of age and composition for a grid with $\eta_R = 0.7$ and $\Delta Y/\Delta Z = 3$, somewhat higher values than typically assumed in the other studies mentioned above. The color-age relation is nonmonotonic. Far-UV light reaches a minimum at about 5 Gyr, after the decay of the warm main sequence and before the EHB channel is well-filled. PAGB stars are always present but are significant in the UV light only for ages $\lesssim$5–10 Gyr, after which the EHB and post-EHB phases dominate. The EHB/post-EHB channel becomes strongly occupied only when the turnoff mass becomes small enough that the assumed RGB mass loss yields small-envelope ZAHB stars. In Figure 10 this occurs after $\sim$16 Gyr for $Z_\odot$ and $\sim$8 Gyr for 3 $Z_\odot$, yielding 1500–V $\lesssim 3$. These threshold ages would decrease by about 5 Gyr for $\eta_R = 1$ (Yi et al 1997b, Figure 22). Although the detailed age-color relation depends on Z, the color loci for $Z \gtrsim Z_\odot$ nearly superpose, implying that the UV colors cannot be easily used to distinguish Z. Tracks for $\eta_R = 1.0$ reproduce the plotted E galaxy data better than those shown here, although these do encompass the entire color range observed. In particular, the plotted models allow significantly stronger UV-upturns (1500–V $\sim +0.5$ and 1500–2500 ~ -1) than actually observed. As indicated by the labeled points, the observed range of 1500–V (though not 1500–2500) could be produced at $t = 15$ Gyr, $\eta_R = 0.7$ by a change of Z of a factor of 2, with a concomitant change in Y. Alternatively, within the modeling uncertainty, the data could be equally well explained by changes in age at constant abundance or by a correlation between η_R and abundance.

7.2 Inferences About Chemical Abundances and Ages

The evolutionary model sets agree that the observed far-UV fluxes can be produced by old (5–15 Gyr), metal-rich ($Z \sim$ 1–3 $Z_\odot$) populations given favorable, but not unreasonable, assumptions about $\Delta Y/\Delta Z$, η_R, and ΔM_{ENV}. They also agree that changes in Z alone cannot reproduce the Faber correlation, unless it is assumed that $\Delta Y/\Delta Z \gtrsim 2.5$ or that η_R increases with Z (as foreseen by GR). Models based on more conservative assumptions about mass loss require that populations with significant UVX components be older than about 10 Gyr.

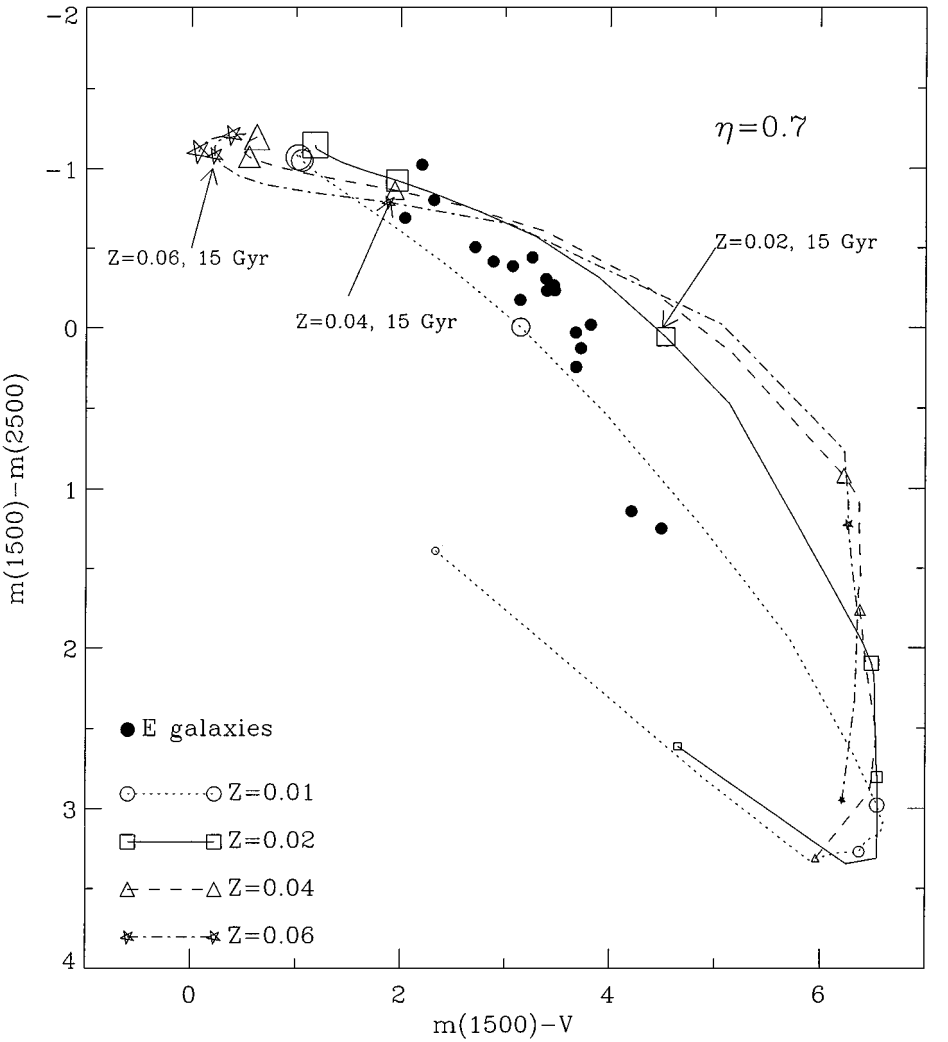

Figure 10 IUE color data (same axes as Figure 7) for E galaxies compared to theoretical models. From Yi et al (1997b). The various symbol shapes correspond to sequences for different Z, as indicated on the legend. The symbol sizes increase with age; the six models in each sequence are for 1, 5, 10, 15, 20, and 25 Gyr. All models assume a Reimers mass-loss parameter of $\eta_R = 0.7$, about twice that estimated for globular clusters. Masses on the ZAHB are assumed to be spread about the mean value (determined by η_R) in a modified Gaussian distribution with $\sigma = 0.06\ M_\odot$. $\Delta Y/\Delta Z$ is assumed to be 3.0. See Section 7.1 for further details.

As noted in Section 6.3 and illustrated in Figure 10, the metal abundance Z, if decoupled from Y and mass loss, has only a secondary influence on the spectrum of the hot components at wavelengths above 1200 Å. There is a somewhat greater effect on the temperature distribution of light in the 900–1200 Å range (Brown et al 1997). Y can have a significant effect on UV flux production, but its influence can be masked by changes in mass loss. Furthermore, the UVX absorption line spectrum is apparently subject to atmospheric diffusion effects, as discovered by Brown et al (1997). Therefore, far-UV spectra in the 1200–2000 Å range cannot easily be used to infer abundances of the hot star populations of E galaxies.

It is also premature to try to use the UVX to age-date elliptical galaxies. The far-UV appears promising for this purpose because it is the most rapidly evolving part of a single-burst galaxy spectrum. A number of studies have noted that the "turn-on" of the UVX (which occurs at the age when M_{TO} drops to the point that the assumed RGB mass loss is able to fill the smaller envelope channels) marks an obvious spectral transition which might be used to age-date E galaxies at moderate lookback times (e.g. GR, Magris & Bruzual 1993, Chiosi 1996, Bressan et al 1996, Chiosi et al 1997, Yi et al 1999). The amplitude of the transition in UV colors is large. Unfortunately, its timing in the models is very sensitive to assumptions about mass loss and helium abundance, making results strongly model-dependent. This can be seen in the cases presented by Yi et al (1997b, 1999).

An interesting related example is the interpretation of the UVX as the product of a metal-poor subpopulation of extremely old (18–20 Gyr) stars, presumably the earliest generation to form in massive galaxies (Lee 1994, Park & Lee 1997). The models employed by Lee and Park adopt atypically small values for both total RGB mass loss (a fixed 0.22 $M_\odot$) and ΔM_{ENV} (0.02 $M_\odot$). Larger values for these parameters would significantly reduce the inferred ages. The models also do not fit the UVX spectra very well, having the flatter energy distributions for 1500–3500 Å characteristic of metal poor systems (Park & Lee 1997), even when mixed metallicities and larger effective mass loss are included (Yi et al 1999).

It is clear in general that assumptions about η_R and ΔM_{ENV} largely determine the outcome of the far-UV evolutionary synthesis models developed to date and any conclusions about t, Y, or Z that may emerge from them. This is necessarily so, given the circumstance that changes in only a few 0.01 $M_\odot$ in M_{ENV} can radically affect the UV output of stars. Age and mass loss can be traded for one another, and without a more deterministic theory of mass loss, derived ages are not reliable.

These remarks apply to the far-UV, hot-star spectra of old populations. The situation is quite different in the mid-UV region (2400–3200 Å) where the light becomes dominated by cool stars ($T_e \sim$ 5500–7500 K) near the main sequence turnoff. Turnoff light is directly sensitive to both age and abundance, whereas red giant light, which is important longward of 4500 Å, is insensitive to age. The principal obstacle to exploitation of the mid-UV as a population diagnostic is the lack of good "libraries" of mid-UV stellar energy distributions. Empirical datasets (e.g. Fanelli et al 1992) tend to be limited to solar abundance, whereas theoretical ones (e.g. Kurucz 1991) have serious shortcomings due to difficulties in treating the

overwhelming UV line blanketing. HST is beginning to fill the gap, if slowly, with high quality, medium-resolution spectra (e.g. Heap et al 1998). Another technical difficulty with the mid-UV is that contamination by the long-wavelength tail of the UVX energy distribution must be removed. Although this contributes over 50% of the 2700 Å light in many cases (BBBFL, Ponder et al 1998), correction for the UVX component is straightforward because it has a smooth and well-determined shape (Dorman et al 1999).

Preliminary synthesis models of the mid-UV using theoretical stellar spectra confirm the expectation that it will be an excellent age/abundance diagnostic. DOR's experiments with fitting broad-band UV colors of E galaxies showed that 2500–V yields much more information on age and composition than does 1500–V. They estimate that $\partial(2500\text{–V})/\partial \log Z \sim 2.7$ for old populations, a much higher sensitivity than for most optical-IR indices (e.g. Worthey 1994). The mid-UV continuum is especially useful in placing limits on the contribution of metal-poor populations to galaxy light. The available mid-UV models show, for instance, that the metal-poor fraction in E galaxies is much smaller than predicted by simple "closed box" nucleosynthetic models (e.g. Tantalo et al 1996, Worthey et al 1996). Empirically, mid-UV spectral features also strongly distinguish the populations of globular clusters and E galaxy cores from one another (e.g. Ponder et al 1998).

One of the most important applications of mid-UV stellar population analysis will be to the spectra of high redshift galaxies. Age-dating of distant objects that are passively evolving, such as LBDS 53W091, with $z = 1.55$, can constrain the earliest epoch of star formation, and hence cosmology (e.g. Spinrad et al 1997).

7.3 Resolved UV Star Populations

The HST has sufficient sensitivity to probe directly the UV star populations of nearby galaxies. Three UV imaging studies of hot stars in M31 and M32, all based on FOC observations of small fields, have appeared to date (King et al 1992, Bertola et al 1995, Brown et al 1998a). Although the two earlier studies suffered from serious calibration difficulties (see Brown et al 1998a), all three detected UV-bright stars and agree that luminous PAGB stars cannot account for more than a small fraction of the total FUV light. The photometry of Brown et al (1998a) has a detection limit of $m_\lambda(1750\ \text{Å}) \sim 24.5$, which is not deep enough to reach the HB itself but does encompass PAGB, PEAGB and AGB-manqué luminosities. Brown and colleagues identify a large number of stars consistent with expectations for the descendants of EHB stars with $M_{ENV} \sim 0.002$–$0.05\ M_\odot$. However, most of the UV light is produced by unresolved stars, presumably on the EHB. The integrated HUT or IUE spectra are consistent with models, normalized by the resolved samples, in which only 2% of the total population passes through the EHB channel in M31 and only 0.5% does so in M32. The lifetime of the PAGB channel, which makes up the rest of the post-HB population, is so short that few resolved objects are expected in the observed fields. Somewhat unexpectedly, the shapes of the luminosity functions for the resolved stars in M31 and M32 are

similar (despite significant differences in optical absorption line spectra). M32 differs only in having fewer total stars (per unit UV surface brightness) above the detection threshold. Brown and coworkers also find that about 10% of the brighter resolved population is not explainable by existing post-HB evolutionary tracks.

Any process that reduces HB envelope masses in a significant fraction of the population can have influence extending beyond the UV region. EHB stars do not become AGB stars, and if most of the evolving population passes through the small-envelope channel, the AGB contribution to the integrated optical/IR spectrum (mainly longward of 6000 Å) of a galaxy will decrease. Changes in the AGB should also be detectable with the surface brightness fluctuation imaging method (Tonry & Schneider 1988). Ferguson & Davidsen (1993) find that the incidence of planetary nebulae, which should also decrease if the AGB population decreases, is anticorrelated with bluer 1500–V colors. This is important circumstantial evidence that small-envelope HB stars are implicated in the UVX. The correlation should be pursued with a larger sample of galaxies, and radial dependences within galaxies should be studied as well.

The existing deep imaging studies therefore provide good support for the EHB interpretation of the UVX. Imaging to the level of the EHB itself within the Local Group can probably be secured with HST/STIS and HST/ACS. Worthey (1993) has described how the surface brightness fluctuation technique can be applied to faint hot stars to extend the effective depth of such UV imaging.

7.4 Cosmic Evolution of the UVX

Since the models predict that the UVX (if dominated by the EHB or PAGB channels) should decrease as the main-sequence turnoff mass increases, there should be strong evolution of the UVX with lookback time (see Section 7.2). If E galaxies are sufficiently homogeneous, there could be a unique lookback beyond which the UVX disappears. Given the uncertainty in the models discussed above, lookback effects should probably be viewed for the present more as a valuable opportunity to refine the models than as a way to age-date the universe.

There are serious technical challenges in making restframe UV measurements at moderate redshifts. The galaxies are faint. At a redshift of 0.5 (a lookback time of 6 Gyr), the distance modulus is 43, implying that the unevolving UVX of a strong upturn source in a typical luminous elliptical would have $m_\lambda(2250\ \text{Å}) \sim 24.5$. Simple detection of far-UV light (e.g. in broad bands) is not sufficient to distinguish a UVX component from the decaying initial burst or late star formation (see Section 5). Multiband photometry or spectroscopy is necessary. Several attempts to observe the UVX at high redshift have been made (e.g. Windhorst et al 1994), but only recently has a detection been claimed in the cluster Abell 370 ($z = 0.38$) by Brown et al (1998b). Using broad-band filters with HST/FOC, they find four cluster E galaxies to have a range of 1500–V similar to that in local galaxies. If this is UVX light, it implies a high formation redshift ($z_F > 4$) in the context of most existing models. An absence of UV evolution over the past few Gyr would

be inconsistent with some classes of UVX models. It will be especially important to link changes in the UVX of distant galaxies with evolution of the initial burst at optical/IR wavelengths (now detected up to $z \sim 0.9$, e.g. Stanford et al 1998).

7.5 Summary and Key Issues

Progress on the UVX problem during the last ten years has been excellent. The theoretical, spectral, and imaging evidence has recently converged toward the view that the UVX originates from He-burning, extreme horizontal branch stars, their post-HB progeny, and post-AGB stars in the dominant, metal-rich stellar population of E galaxies. The mixture of these types apparently varies from object to object, perhaps in a systematic way with global mean metallicity or mass, but in most cases the EHB/post-EHB channels are the more important. The simplest explanation for the correlation between the UVX and optical line strengths is that the mass-loss parameter η_R increases with Z or that $\Delta Y/\Delta Z \gtrsim 2.5$.

Although evolutionary synthesis models successfully predict UV spectral properties in the ranges observed, progress in understanding the UVX, and in refining estimates of ages and abundances derived therefrom, is hampered by our lack of knowledge of two basic processes: mass loss on the giant branch and helium enrichment. Both of these are critical to the efficiency with which an old population can generate UV-bright stars. We urgently require a more complete and predictive physical theory of giant-branch mass loss. This is the highest priority for UVX theory in the near term. The question of the value of the helium enrichment parameter ($\Delta Y/\Delta Z$) near and above solar abundance also needs to be addressed. Both areas demand extensive observational programs on nearby systems as well as fundamental improvements in theoretical modeling. The same is true of diffusion in hot atmospheres, which is important to interpreting the UVX line spectrum.

These are the most serious gaps in our astrophysical understanding of the UVX, but there are other troublesome issues as well, three of which are worth mentioning:

1. The behavior of the UVX seems to be firmly linked to that of the lighter elements such as N, Mg, and Na and decoupled from the Fe-peak (Section 5.2). This adds an additional dimension to modeling space, so far unexplored, which is not at present well supported by nucleosynthetic theory (Worthey 1998).
2. The internal spatial gradients in 1500–B color discussed in Section 4.2 do not correlate with gradients in Mg_2 (Ohl et al 1998). Metallicity is evidently not the sole parameter governing the UVX. This may be related to the decoupling of the Fe-peak noted in paragraph 1 above, or it may reflect the influence of other changing parameters within galaxies, such as age or Y abundance. M32, with a large and reversed UVX gradient (see Figure 3), is an important case since there is considerable independent evidence for an intermediate age ($\lesssim$8 Gyr) population there and possibly an age gradient in which the central regions are younger (O'Connell 1980, Freedman 1992, Rose 1994, Hardy et al 1994, Faber et al 1995, Grillmair et al 1996).

3. There has been very little work on the dependence of the UVX on galaxy morphology despite suggestions of differences between E galaxies and S0 galaxies (e.g. Smith & Cornett 1982). Bright, nearby spiral bulges could readily be studied in the UV with HST, and comparisons with E galaxies could help distinguish some of the underlying drivers of the UVX phenomenon. If, for example, bulges have a wider range of ages than E galaxies (e.g. Wyse et al 1997), then the younger ones should have smaller UV upturns than E's.

8. OTHER FAR-UV PHENOMENA IN E GALAXIES

Although the UVX produces a ubiquitous extended light background in old populations, it is at a low level and is coincident with a "dark window" in the natural sky background centered at about 2000 Å, where the sky is about 40× fainter than at any other wavelength in the optical-IR region (O'Connell 1987). The faint UV backgrounds permit isolation of other interesting phenomena that are either unique to the UV or are drowned out in the visible bands by the glare of the main sequence and giant branch stars. This includes low-luminosity active nuclei, recent star formation, blue straggler populations, gas in the 10^5–10^6 K temperature range, scattered light from dust grains, and H_2 fluorescence features near 1600 Å. As noted in Section 3, hot continuum sources that contribute as little as 0.1% of the V-band light of a galaxy can be readily detected in the UV region. In this section we briefly discuss UV observations relevant to massive star formation and nonthermal nuclei.

Recent Massive Star Formation Identification of a minority component of massive stars in an old population depends on detection of spectral or color distortions in integrated light or on imaging of individual stars or concentrations of stars that stand out against the smooth background light. The vacuum UV is about 30–50× more sensitive to such effects than the optical/IR bands (McNamara & O'Connell 1989). Based on spectral synthesis models for constant star formation with a normal IMF (e.g. Bruzual & Charlot 1993, Cornett et al 1994), the star formation rate per unit V-band luminosity is related to far-UV color as follows:

$$\dot{S}/L_V \sim 8 \times 10^{-11}\, 10^{-0.4(1500-V)}\, \mathrm{M}_\odot\ \mathrm{yr}^{-1}\, L_{V,\odot}^{-1}.$$

The 1500 Å flux used to compute the color here is the part of the total far-UV flux that is attributed to young stars. The coefficient in this expression is almost independent of the period over which the star formation is assumed to have persisted, for periods over 50 Myr.

If all of the UV light in the strongest UV upturn cases (1500–V $\sim$ 2) were attributed to massive star formation, the implied normalized rate would be $\dot{S}/L_V \sim 1.3 \times 10^{-11}$, or a total rate of $\dot{S} \sim 0.25\ \mathrm{M}_\odot\ \mathrm{yr}^{-1}$ for a typical gE galaxy with $M_V = -21$. This is obviously a strong upper limit to massive star formation in a normal E galaxy since only a small fraction of the far-UV light can be produced

by massive stars, as discussed in detail in Sections 4 and 5. If we take 20% as the upper limit on the contribution of young starlight at 1500 Å in a galaxy with a more typical UV upturn with 1500–V = 3.5, then the maximal total rate becomes $\dot{S} \lesssim 0.01$ $M_\odot$ yr^{-1}. This is a very stringent limit on the amount of continuing star formation in a typical gE galaxy.

These values can be compared with the estimated total mass loss from stars evolving up the giant branch. The "evolutionary rate" in an old population (i.e. the number of stars evolving off the main sequence per unit time) is $\sim 4 \times 10^{-11}$ yr^{-1} $L_{V,\odot}^{-1}$ (e.g. Renzini & Buzzoni 1986, DOR). If each star sheds 0.3–0.5 $M_\odot$, then the total estimated normalized mass loss rate is $\dot{m}/L_V \sim 1$–2×10^{-11} $M_\odot$ yr^{-1} $L_{V,\odot}^{-1}$, or 0.2–0.4 $M_\odot$ yr^{-1} for a galaxy with $M_V = -21$. The maximal continuing star formation rate derived from far-UV data is some 20–40× smaller. Clearly, most of the material produced by giant branch mass loss is not being recycled into new stars in normal E galaxies, at least not with a normal IMF. The UV is the key to this conclusion, since high S/N optical-band studies generally cannot exclude complete recycling (e.g. O'Connell 1980, Gunn et al 1981).

The ultimate fate of the lost red giant envelopes remains unclear. At early times the material is probably removed from galaxy interiors by high-temperature, supernovae-driven winds. In more massive galaxies, the gas forms a hot corona, which is detectable at X-ray wavelengths (e.g. Forman et al 1985). Some fraction of the corona is returned to the interior by a cooling flow (e.g. Sarazin & White 1988, David et al 1991), but the final repository of the material from the flow remains to be identified. One interesting example of young stars in a normal old population is the remarkable source P2, which is coincident with the dynamical center of M31 (King et al 1995, Lauer et al 1998). This is slightly extended and considerably bluer than the surrounding UVX population. It has the characteristics of an intermediate-age star cluster, but with $M_V = -5.7$, it can account for only a tiny fraction of recent mass loss by the bulge giants. Its massive stars may have been formed through stellar collisions. The second concentrated nuclear source in M31, denoted P1, is not at the dynamical center and is brighter at optical wavelengths. However, its UV properties are similar to those of the inner bulge. It has been suggested that this is a cannibalized galaxy nucleus in the final stages of consumption by M31. If so, it has managed to clothe itself with a UVX population similar to the bulge stars in M31.

The minority of nearby early-type galaxies that do exhibit evidence for recent star formation (including NGC 205, 5102, and 5253) have probably mostly suffered gas transfer during a recent interaction. UV observations in these cases provide a much improved picture of the massive star population and its history than do optical data (e.g. BBBFL, Wilcots et al 1990, Deharveng et al 1997, Calzetti et al 1997). By contrast with normal E galaxies, recent star formation is often found in early-type galaxies associated with massive cluster cooling flows (reviewed in Fabian 1994). Systems with UV observations include M87, Abell 2199, and NGC 1275 (Perola & Tarenghi 1980, Bertola et al 1982, Bertola et al 1986, BBBFL, McNamara & O'Connell 1989, Smith et al 1992, Dixon et al 1996). The UV is

important here in placing better limits on star formation rates (always much smaller than X-ray estimates of total accretion rates) and in exploring possible anomalies in the initial mass function.

Active Nuclei The flat energy distributions of nuclear nonthermal sources imply that the contrast of an AGN against its surroundings in an E galaxy can improve by a factor up to ∼100 in the UV compared with the optical-IR. This permits better study of known nuclei and searches for very low-luminosity activity. A number of identifications of nuclear point sources have recently been made by UV imaging either of complete samples of nearby galaxies (Maoz et al 1995, 1996) or of samples of objects with Low Ionization Nuclear Emission Region (LINER) optical spectra (Barth et al 1998). Only about 30% of the known LINERs are detected this way, and Maoz and Barth and their respective colleagues suggest that obscuration by dust reduces the visibilty of the other nuclei, at least in the disk galaxies in their samples. However, the UV brightnesses of the nonthermal nuclei support photoionization (rather than shock excitation) models for the LINER emission lines.

In the case of E galaxies with known bright nuclei (e.g. M87), the AGN contributes only a small part of the FUV light within the IUE aperture. From the UIT images of Ohl et al (1998), we find that the nucleus and jet in M87 produce only 10% of the FUV light within a radius of 10". A similar situation applies to NGC 4278, whose nonthermal nucleus was recently detected by Moller et al (1995). These amounts are, however, sufficient to shift the active galaxies such as M87, NGC 4278, and NGC 1052 slightly in 1500–V vs Mg_2 diagrams such as Figure 6 (as first remarked by BBBFL).

The most interesting case of UV-facilitated observations of an E galaxy AGN is that of NGC 4552. This object has conspicuous radio and infrared signatures of an active nucleus and was originally observed with IUE for that reason (O'Connell et al 1986). Aside from a strong, spatially extended UV-upturn, however, there were no nuclear anomalies obvious until HST imaging was obtained by Renzini et al (1995) and Cappellari et al (1998). The HST observations show a time-variable, unresolved ($r \lesssim 0.07$") spike of UV light which brightened by a factor of 4.5× between 1991 and 1993. Without the resolution of HST and the improved contrast offered by the UV, it would have been impossible to detect this source, which is currently the least luminous known AGN, having an Hα luminosity of only 6×10^{37} erg s^{-1}. The outburst probably corresponds to the accretion of material stripped from a single star during a close fly-by of the nuclear black hole (Cappellari et al 1998).

9. CONCLUSION

Ultraviolet observations have opened a new, and unexpectedly rich, window on old stellar populations that has revealed phenomena that are either difficult or impossible to study at longer wavelengths. The identification of the UVX component

with low-mass, small-envelope stars has led to the recognition that the spectra of distant E galaxies are remarkably sensitive to what in traditional stellar population research would have been regarded as subtle astrophysical processes, including giant-branch mass loss, helium enrichment, and atmospheric diffusion. The fact that these processes are manifestly not properly understood at the moment, precluding a definitive interpretation of the UVX in terms of global population parameters, is less important than the long-term promise of UV observations as powerful probes of galaxy evolution.

ACKNOWLEDGMENTS

For comments, figures, and other help in preparing this paper, I am most grateful to Ralph Bohlin, Tom Brown, Dave Burstein, Daniela Calzetti, Jeff Crane, Ben Dorman, Harry Ferguson, Ian Freedman, Richard de Grijs, Wayne Landsman, Ray Ohl, Alvio Renzini, Bob Rood, Ted Stecher, and Sukyoung Yi. This work has been supported in part by NASA Long Term Space Astrophysics grant NAG5-6403.

LITERATURE CITED

Baade W. 1944. *Ap. J.* 100:137–46
Bailyn CD. 1995. *Annu. Rev. Astron. Astrophys.* 33:133–62
Barbaro G, Olivi FM. 1989. *Ap. J.* 337:125–40
Barth AJ, Ho LC, Filippenko AV, Sargent WLW. 1998. *Ap. J.* 496:133–44
Bender R. 1988. *Astron. Astrophys. Lett.* 193: L7–10
Bertelli G, Bressan A, Chiosi C, Fagotto F, Nasi E. 1994. *Astron. Astrophys. Suppl.* 106:275–302
Bertelli G, Chiosi C, Bertola F. 1989. *Ap. J.* 339: 889–903
Bertola F, Bressan A, Burstein D, Buson LM, Chiosi C, Di Serego Alighieri S. 1995. *Ap. J.* 438:690–94
Bertola F, Capaccioli M, Holm AV, Oke JB. 1980. *Ap. J.* 237:L65–69
Bertola F, Capaccioli M, Oke JB. 1982. *Ap. J.* 254:494–99
Bertola F, Gregg MD, Gunn JE, Oemler A. 1986. *Ap. J.* 303:624–28
Bica E, Alloin D. 1988. *Astron. Astrophys.* 192: 98–106
Bica E, Bonatto C, Pastoriza MG, Alloin D. 1996. *Astron. Astrophys.* 313:405–16
Blöcker T, Schönberner D. 1990. *Astron. Astrophys. Lett.* 240:L11–14
Bohlin RC, Cornett RH, Hill JK, Hill RS, O'Connell RW, Stecher TP. 1985. *Ap. J. Lett.* 298:L37–40
Boksenberg A, Evans RG, Fowler RG, Gardner ISK, Houziaux L, et al. 1973. *MNRAS* 163: 291–322
Boggess A, Wilson R. 1987. In *Exploring the Universe with IUE*, ed. Y Kondo pp. 3–20. Dordrecht: Reidel
Bowen GH, Willson LA. 1991. *Ap. J. Lett.* 375:L53–56
Bressan A, Chiosi C, Fagotto F. 1994. *Ap. J. Suppl.* 94:63–115
Bressan A, Chiosi C, Tantalo R. 1996. *Astron. Astrophys.* 311:425–45
Brocato E, Matteucci F, Mazzitelli I, Tornambé A. 1990. *Ap. J.* 349:458–70
Brosch N. 1998, *Exp. Astron.* In press
Brown TM, Ferguson HC, Davidsen AF. 1995. *Ap. J. Lett.* 454:L15–18
Brown TM, Ferguson HC, Davidsen AF, Dorman B. 1997. *Ap. J.* 482:685–707

Brown TM, Ferguson HC, Stanford SA, Deharveng JM. 1998a. *Ap. J.* 504:113–38

Brown TM, Ferguson HC, Deharveng JM, Jedrzejewski RI. 1998b. *Ap. J. Lett.* 508:L139–42

Bruzual AG, Charlot S. 1993. *Ap. J.* 405:538–53

Buonanno R, Corsi C, Bellazzini M, Ferraro FR, Fusi Pecci F. 1997. *Astron. J.* 113:706–12

Burstein D, Bertola F, Buson LM, Faber SM, Lauer TR. 1988. *Ap. J.* 328:440–62. (BBBFL)

Burstein D, Faber SM, Gaskell CM, Krumm N. 1984. *Ap. J.* 287:596–609

Caloi V. 1989. *Astron. Astrophys.* 221:27–35

Calzetti D, Meurer GR, Bohlin RC, Garnett DR, Kinney AL, et al. 1997. *Astron. J.* 114:1834–49

Cappellari M, Renzini A, Greggio L, di Serego Alighieri L, Buson M, et al. 1998. *Ap. J.* In press

Carruthers GR, Heckathorn HM, Opal CB. 1978. *Ap. J.* 225:346–56

Castellani V, Cassatella A. 1987. In *Exploring the Universe with the IUE Satellite*, ed. Y Kondo, pp. 637–54. Dordrecht: Reidel

Castellani M, Castellani V. 1993. *Ap. J.* 407: 649–56

Castellani M, Castellani V, Pulone L, Tornambé A. 1994. *Astron. Astrophys.* 282:771–74

Castellani M, Limongi M, Tornambé A. 1992. *Ap. J.* 389:227–33

Castellani M, Tornambé A. 1991. *Ap. J.* 381: 393–408

Chiosi C. 1996. In *From Stars to Galaxies: The Impact of Stellar Physics on Galaxy Evolution*, eds. C Leitherer, U Fritze-von Alvensleben, J Huchra, 98:181–92. San Francisco: Astron. Soc. Pacific

Chiosi C, Vallenari A, Bressan A. 1997. *Astron. Astrophys. Suppl.* 121:301–19

Ciardullo RB, Demarque P. 1978. In *The HR Diagram*, eds. AG Davis Philip, DS Hayes, (IAU Symposium No 80), pp. 345–48. Dordrecht: Reidel

Code AD. 1969. *Publ. Astron. Soc. Pac.* 81: 475–87

Code AD, Welch GA. 1981. *Ap. J.* 228:95–104

Code AD, Welch GA. 1982. *Ap. J.* 256:1–12

Code AD, Welch GA, Page T. 1972. In *Scientific Results from the Orbiting Astronomical Observatory*, ed. AD Code (NASA SP-310), pp. 559–74

Cole AA, Gallagher JS, Mould JR, Clarke JT, Trauger JT, et al. 1998. *Ap. J.* 505:230–35

Coleman GD, Wu CC, Weedman DW. 1980. *Ap. J. Suppl.* 43:393–416

Cornett RH, O'Connell RW, Greason MR, Offenberg JD, Angione RJ, et al. 1994. *Ap. J.* 426:553–62

Crenshaw DM, Breugman OW, Normal DJ. 1990. *Publ. Astron. Soc. Pac.* 102:463–77

David L, Forman W, Jones C. 1991. *Ap. J.* 369:121–34

Davidsen AF, Ferguson HC. 1992. In *Physics of Nearby Galaxies: Nature or Nurture?*, eds. TX Thuan, C Balkowski, JTT Van, pp. 125–37. Paris: Editions Frontieres

D'Cruz NL, Dorman B, Rood RT, O'Connell RW. 1996. *Ap. J.* 466:359–71

Dean CA, Bruhweiler FC. 1985. *Ap. J. Suppl.* 57:133–43

de Boer KS. 1982. *Astron. Astrophys. Suppl.* 50:247–50

de Boer KS. 1985. *Astron. Astrophys.* 142:321–32

de Boer KS. 1987. In *The Second Conference on Faint Blue Stars*, eds. AGD Philip, DS Hayes, JW Liebert, (IAU Colloquium No 95), pp. 95–104. Schenectady, NY: L Davis Press

Deharveng JM, Jakobsen P, Milliard B, Laget M. 1980. *Astron. Astrophys.* 88:52–57

Deharveng JM, Jedrzejewski R, Crane P, Disney MJ, Rocca-Volmerange B. 1997. *Astron. Astrophys.* 326:528–36

Deharveng JM, Joubert M, Monnet G, Donas J. 1982. *Astron. Astrophys.* 106:16–20

Deharveng JM, Laget M, Monnet G, Vuillemin A. 1976. *Astron. Astrophys.* 50:371–75

Deharveng JM, Sasseen TP, Buat V, Bowyer S, Lampton M, Wu X. 1994. *Astron. Astrophys.* 289:715–28

Dixon WVD, Davidsen AF, Ferguson HC. 1996. *Astron. J.* 111:130–39
Donas J, Milliard B, Laget M. 1995. *Astron. Astrophys.* 303:661–72
Dorman B. 1992. *Ap. J. Suppl.* 81:221–50
Dorman B, O'Connell RW, Rood RT. 1995. *Ap. J.* 442:105–41. (DOR)
Dorman B, O'Connell RW, Rood RT. 1999. In preparation
Dorman B, Rood RT, O'Connell RW. 1993. *Ap. J.* 419:596–614
Dorman B, Shah RY, O'Connell RW, Landsman WB, Rood RT, et al. 1997. *Ap. J. Lett.* 480:L31–34
Dupree AK. 1986. *Annu. Rev. Astron. Astrophys.* 24:377–420
Faber SM. 1983. *Highlights of Astronomy* 6: 165–71
Faber SM, Trager SC, Gonzalez JJ, Worthey G. 1995. In *Stellar Populations*, ed. P van der Kruit, G Gilmore. IAU Symposium 164, pp. 249–57. Dordrecht: Kluwer
Faber SM, Tremaine S, Ajhar EA, Byun YI, Dressler A, et al. 1997. *Astron. J.* 114:1771–96
Fabian AC. 1994. *Annu. Rev. Astron. Astrophys.* 32:277–318
Fanelli MN, O'Connell RW, Burstein D, Wu CC. 1992. *Ap. J. Suppl.* 82:197–245
Ferguson HC, Davidsen AF, Kriss GA, Blair WP, Bowers CW, et al. 1991. *Ap. J.* 382:L69–73
Ferguson HC, Davidsen AF. 1993. *Ap. J.* 408: 92–107
Ferraro FR, Paltrinieri B, Fusi Pecci F, Rood RT, Dorman B. 1998. *Ap. J.* 500:311–19
Forman W, Jones C, Tucker W. 1985. *Ap. J.* 293:102–19
Freedman WL. 1992. *Astron. J.* 104:1349–59
Fusi Pecci F, Ferraro FR, Bellazzini M, Djorgovski S, Piotto G, Buonanno R. 1993. *Astron. J.* 105:1145–68
Gallagher JS. 1972. *Astron. J.* 77:568–72
Gingold RA. 1976. *Ap. J.* 204:116–30
Green EM. 1999. In *3rd Conference on Faint Blue Stars*, ed. AGD Philip. Schenectady: Davis. In press
Greenstein JL, Sargent AI. 1974. *Ap. J. Suppl.* 28:157–200
Greggio L, Renzini A. 1990. *Ap. J.* 364:35–64. (GR)
Greggio L, Renzini A. 1999. In "UV Astronomy in Italy," ed LM Buson, D DeMartino. *Mem. S. A. Italia*. In press
Grillmair CJ, Lauer TR, Worthey G, Faber SM, Freedman WL, et al. 1996. *Astron. J.* 112: 1975–87
Gunn JE, Stryker LL, Tinsley BM. 1981. *Ap. J.* 249:48–67
Hardy E, Couture J, Couture C, Joncas G. 1994. *Astron. J.* 107:195–205
Heap SR, Brown TM, Hubeny I, Landsman W, Yi S, et al. 1998. *Ap. J. Lett.* 492:L131–34
Heber U. 1992. In *Atmospheres of Early-Type Stars*, ed. U Heber, CS Jeffrey, p. 233. Berlin: Springer
Hills JG. 1971. *Astron. Astrophys.* 12:1–4
Horch E, Demarque P, Pinsonneault M. 1992. *Ap. J. Lett.* 388:L53–56
Iben I, Rood RT. 1970. *Ap. J.* 161:587–617
Izotov YI, Thuan TX. 1998. *Ap. J.* 500:188–216
Jaffe W, Ford HC, O'Connell RW, van den Bosch F, Ferrarese L. 1994. *Astron. J.* 108: 1567–78
Johnson HM. 1979. *Ap. J. Lett.* 230:L137–40
Jørgensen UG, Thejll P. 1993. *Ap. J. Lett.* 411: L67–70
Joseph CL. 1995. *Exp. Astron.* 6:97–127
Kaluzny J, Rucinski SM. 1995. *Astron. Astrophys. Suppl.* 114:1–20
Kent SM. 1983. *Ap. J.* 266:562–67
King CR, Ellis RS. 1985. *Ap. J.* 288:456–64
King IR, Deharveng JM, Albrecht R, Barbieri C, Blades JC, et al. 1992. *Ap. J. Lett.* 397: L35–38
King IR, Stanford SA, Crane P. 1995. *Astron. J.* 109:164–72
Kinney AL, Bohlin RC, Calzetti D, Panagia N, Wyse RFG. 1993. *Ap. J. Suppl.* 86:5–93
Kinney AL, Calzetti D, Bohlin RC, McQuade K, Storchi-Bergmann T, Schmitt HR. 1996. *Ap. J.* 467:38–60

Kodaira K, Watanabe T, Onaka T, Tanaka W. 1990. *Ap. J.* 363:422–34

Kondo Y, ed. 1987. *Exploring the Universe with the IUE Satellite.* Dordrecht: Reidel. 787 pp.

Kruk JW, Durrance ST, Kriss GA, Davidsen AF, Blair WP, Espey BR. 1995. *Ap. J. Lett.* 454:L1–4

Kurucz RL. 1991. In *Precision Photometry: Astrophysics of the Galaxy*, ed. AGD Philip, AR Upgren, KA Janes, pp. 27–44. Schenectady: Davis

Landsman WB, Bohlin RC, Neff SG, O'Connell RW, Roberts MS, et al. 1998. *Astron. J.* 116:789–800

Landsman WB, Sweigart AV, Bohlin RC, Neff SG, O'Connell RW, et al. 1996. *Ap. J. Lett.* 472:L93–96

Lauer TR, Faber SM, Ajhar EA, Grillmair CJ, Scowen PA. 1998. *Astron. J.* 116:2263–86

Lee YW. 1994. *Ap. J. Lett.* 430:L113–16

Liebert J, Saffer RA, Green EM. 1994. *Ap. J.* 107:1408–21

Longo G, Capaccioli M, Bender R, Busarello G. 1989. *Astron. Astrophys. Lett.* 225:L17–19

Magris G, Bruzual G. 1993. *Ap. J.* 417:102–11

Maoz D, Filippenko AV, Ho LC, Macchetto FD, Rix HW, Schneider DP. 1996. *Ap. J. Suppl.* 107:215–26

Maoz D, Filippenko AV, Ho LC, Rix HW, Bahcall JN, et al. 1995. *Ap. J.* 440:91–99

Martin C, Friedman P, Schiminovich D, Madore B, Bianchi L, et al. 1997. *Bull. Amer. Astron. Soc.* 191:#63.04

McNamara BR, O'Connell RW. 1989. *Astron. J.* 98:2018–43

McWilliam A. 1997. *Annu. Rev. Astron. Astrophys.* 35:503–56

Mengel JG, Norris J, Gross PG. 1976. *Ap. J.* 204:488–92

Milliard B, Donas J, Laget M, Armand C, Vuillemin A. 1992. *Astron. Astrophys.* 257: 24–30

Minkowski R, Osterbrock D. 1959 *Ap. J.* 129: 583–595

Moller P, Stiavelli M, Zeilinger WW. 1995. *MNRAS* 276:979–1002

Nesci R, Perola GC. 1985. *Astron. Astrophys.* 145:296–304

Nörgaard-Nielsen HU, Kjærgaard P. 1981. *Astron. Astrophys.* 93:290–96

O'Connell DJK, ed. 1958. *Stellar Populations*, Amsterdam: North Holland. 544 pp.

O'Connell RW. 1976. *Ap. J.* 206:370–90

O'Connell RW. 1980. *Ap. J.* 236:430–40

O'Connell RW. 1987. *Astron. J.* 94:876–82

O'Connell RW. 1991. *Adv. Space Research* 11 No. 11:71–80

O'Connell RW, Bohlin RC, Collins NR, Cornett RH, Hill JK, et al. 1992. *Ap. J. Lett.* 395:L45–L48

O'Connell RW, Dorman B, Shah RY, Rood RT, Landsman WB, et al. 1997. *Astron. J.* 114: 1982–91

O'Connell RW, Thuan TX, Puschell JJ. 1986. *Ap. J. Lett.* 363:L37–L40

Ohl RG, O'Connell RW, Bohlin RC, Collins NR, Dorman B, et al. 1998. *Ap. J. Lett.* 505: L11–L14

Oke JB, Bertola F, Capccioli M. 1981. *Ap. J.* 243:453–59

Onaka T, Tanaka W, Watanabe T, Watanabe J, Yamaguchi A, et al. 1989. *Ap. J.* 342:238–49

Park JH, Lee YW. 1997. *Ap. J.* 476:28–39

Peletier RF, Davies RL, Illingworth GD, Davis LE, Cawson M. 1990. *Astron. J.* 100:1091–1142

Pence W. 1976. *Ap. J.* 203:39–51

Perola GC, Tarenghi M. 1980. *Ap. J.* 240:447–54

Ponder J, Burstein D, O'Connell RW, Rose J, Frogel JA, et al. 1998. *Astron. J.* 116:2297–314

Renzini A. 1981a. *Ann. Phys. Fr.* 6:87–102

Renzini A. 1981b. In *Effects of Mass Loss on Stellar Evolution*, eds. C Chiosi, R Stalio. pp. 319–38. Dordrecht: Reidel

Renzini A, Buzzoni A. 1986. In *Spectral Evolution of Galaxies*, eds. C Chiosi, A Renzini, pp. 195–235. Dordrecht: Reidel

Renzini A, Greggio L, di Serego Alighieri S, Cappellari M, Burstein D, Bertola F. 1995. *Nature* 378:39–41

Rich RM, Sosin C, Djorgovski SG, Piotto G,

King IR, et al. 1997. *Ap. J. Lett.* 484:L25–28
Rifatto A, Longo G, Capaccioli M. 1995a. *Astron. Astrophys. Suppl.* 109:341–45
Rifatto A, Longo G, Capaccioli M. 1995b. *Astron. Astrophys. Suppl.* 114:527–36
Rocca-Volmerange B, Guiderdoni B. 1987. *Astron. Astrophys.* 175:15–22
Rocca-Volmerange B, Guiderdoni B. 1988. *Astron. Astrophys. Suppl.* 75:93–106
Rood RT. 1973. *Ap. J.* 184:815–38
Rose JA. 1985. *Astron. J.* 90:1927–56
Rose JA. 1994. *Astron. J.* 107:206–29
Rose WK, Tinsley BM. 1974. *Ap. J.* 190:243–51
Saffer RA, Bergeron P, Koester D, Liebert J. 1994. *Ap. J.* 432:351–66
Saffer RA, Liebert J. 1995. In *Proc. of the 9th European Workshop on White Dwarfs*, ed. D Koester, K. Werner, pp. 221–32. Berlin: Springer
Sandage AR, Visvanathan N. 1978. *Ap. J.* 225: 742–50
Sarazin CL, White RE. 1988. *Ap. J.* 331:102–15
Schönberner D. 1983. *Ap. J.* 272:708–14
Smith AM, Cornett RH. 1982. *Ap. J.* 261:1–11
Smith EP, O'Connell RW, Bohlin RC, Cheng KP, Cornett RH, et al. 1992. *Ap. J. Lett.* 395: L49–54
Sosin C, Dorman B, Djorgovski SG, Piotto G, Rich RM, et al. 1997. *Ap. J. Lett.* 480:L35–38
Spinrad H, Dey A, Stern D, Dunlop J, Peacock J, et al. 1997. *Ap. J.* 484:581–601
Stanford SA, Eisenhardt PR, Dickinson M. 1998. *Ap. J.* 492:461–79
Stecher TP, Cornett RH, Greason MR, Landsman WB, Hill JK, et al. 1997. *Publ. Astron. Soc. Pac.* 109:584–99
Sweigart AV. 1987. *Ap. J. Suppl.* 65:95–135
Sweigart AV. 1997. *Ap. J. Lett.* 474:L23–26
Sweigart AV, Mengel JG, Demarque P. 1974. *Astron. Astrophys.* 30:13–19
Tantalo R, Chiosi C, Bressan A, Fagotto F. 1996. *Astron. Astrophys.* 311:361–83
Thejll P, Flynn C, Williamson R, Saffer R. 1997. *Astron. Astrophys.* 317:689–93
Tinsley BM. 1972a. In *Scientific Results from the Orbiting Astronomical Observatory*, ed. AD Code, (NASA SP-310), pp. 575–81
Tinsley BM. 1972b. *Ap. J.* 178:319–36
Tinsley BM. 1980. *Fund. Cosmic Phys.* 5:287
Tonry J, Schneider DP. 1988. *Astron. J.* 96:807–15
Trager SC, Worthey G, Faber SM, Burstein D, González JJ. 1998. *Ap. J. Suppl.* 116:1–28
Treyer MA, Ellis RS, Milliard B, Donas J, Bridges TJ. 1998. *MNRAS* 300:303–14
van Albada TS, de Boer KS, Dickens RJ. 1981. *MNRAS* 195:591–606
Vassiliadis E, Wood PR. 1994. *Ap. J. Suppl.* 92: 125–44
Welch GA. 1982. *Ap. J.* 259:77–88
Whitney JH, O'Connell RW, Rood RT, Dorman B, Landsman WB, et al. 1994. *Astron. J.* 108:1350–63
Whitney JH, Rood RT, O'Connell RW, D'Cruz NL, Dorman B, et al. 1998. *Ap. J.* 495:284–96
Wilcots EM, Hodge P, Eskridge PB, Bertola F, Buson L. 1990. *Ap. J.* 364:87–93
Willson LA, Bowen GH, Struck C. 1996. In *From Stars to Galaxies: The Impact of Stellar Physics on Galaxy Evolution*, eds. C Leitherer, U Fritze-von Alvensleben, J Huchra, 98:197–201. San Francisco: Astron. Soc. Pacific
Windhorst RA, Pascarelle SM, Keel WC, Bertola B, McCarthy PJ, et al. 1994. In *Frontiers of Space and Ground-Based Astronomy*, eds. EW Wamsteker, MS Longair, Y Kondo, pp. 663–67. Dordrecht: Kluwer
Wilson TL, Rood RT. 1994. *Annu. Rev. Astron. Astrophys.* 32:191–226
Worthey G. 1993. *Ap. J. Lett.* 415:L91–94
Worthey G. 1994. *Ap. J. Suppl.* 95:107–49
Worthey G. 1998. *Publ. Astron. Soc. Pac.* 110: 888–99
Worthey G, Dorman B, Jones LA. 1996. *Astron. J.* 112:948–53
Wu CC, Faber SM, Gallagher JS, Peck M, Tinsley BM. 1980. *Ap. J.* 237:290–302
Wu CC, Reichert GA, Ake TB, Boggess A, Holm AV, et al. 1992. *IUE Ultraviolet Spec-*

tral Atlas of Selected Astronomical Objects. (NASA Reference Publication No. 1285).
Wyse RFG, Gilmore G, Franx M. 1997. *Annu. Rev. Astron. Astrophys.* 35:637–75
Yi S, Demarque P, Kim YC. 1997a. *Ap. J.* 482:677–84
Yi S, Demarque P, Oemler A. 1995. *Publ. Astron. Soc. Pac.* 107:273–78
Yi S, Demarque P, Oemler A. 1997b. *Ap. J.* 486:201–29
Yi S, Lee YW, Woo JH, Park JH, Demarque P, Oemler A. 1999. *Ap. J.* 513:128–41

Annual Review of Astronomy and Astrophysics
Volume 37, 1999

CONTENTS